1955

# Magnetic modulator design for a pulsed radar

Howe, Odia E.

# MAGNETIC MODULATOR DESIGN FOR A PULSED RADAR

ODIA E. HOWE, JR.

# MAGNETIC MODULATOR DESIGN

# FOR A

# PULSED RADAR

* * * *

Odia E. Howe, Jr.

(For Official Use Only)

CONTAINS PROPRIETARY INFORMATION.

MAY NOT BE RELEASED TO,
OR FOR THE USE OF, NON-
NAVY ACTIVITIES, WITHOUT
SPECIFIC WRITTEN PERMISSION
OF AUTONETICS (A DIVISION
OF NORTH AMERICAN AVIATION)
9150 E. ~~EE~~ IMPERIAL HIGHWAY
P.O. BOX "AN", BELLFLOWER,
CALIFORNIA

Permission to release denied 5/2/56 — GRL

# MAGNETIC MODULATOR DESIGN

# FOR A PULSED RADAR

by

Odia E. Howe, Jr.

Major, United States Marine Corps

Submitted in partial fulfillment
of the requirements
for the degree of
MASTER OF SCIENCE
IN
ENGINEERING ELECTRONICS

United States Naval Postgraduate School
Monterey, California

1955

This work is accepted as fulfilling

the thesis requirements for the degree of

MASTER OF SCIENCE

IN

ENGINEERING ELECTRONICS

from the

United States Naval Postgraduate School

## PREFACE

One of the primary problems facing modern commanders of military units, whether afloat, ashore, or in the air, is the answer to the question, "Are our electronic devices in operating condition?" This question, in particular, can be asked of our detection devices, which are, in the main, pulsed radar.

A critical component of a pulsed radar is the modulator unit. These units present a difficult maintenance problem in many present day sets due to the difficulty of switching high power, high repetition rate pulses. Failures of these modulator units can usually be attributed to:

1. Failure of vacuum tubes, either thyratron or standard types.
2. Component failure. (Resistors, capacitors, coils)
3. Delay line failure. (Pulse forming networks)

Any steps taken to eliminate the above will contribute to the overall availability of a given unit.

One of the systems developed to accomplish this step has been the development of the magnetic modulator. This unit uses no vacuum tubes, with the lone exception of the magnetron oscillator. Components can be designed with adequate safety factors to markedly reduce component failure. Lastly, there is not a pulse forming network present in the conventional sense. This unit converts a sinusoidal input to a short pulse, and controls the switching of this pulse. In this sense, it could be called a pulse forming network.

It is the aim of this paper to show the mathematical analysis of such a circuit, followed by a typical design to fit radar specifications.

The writer is indebted to Mr. M. F. Thompson and Mr. E. R. Ingersoll, of North American Aviation, Inc., for their assistance and aid in the preparation of this paper.

TABLE OF CONTENTS

LIST OF ILLUSTRATIONS

## TABLE OF SYMBOLS AND ABBREVIATIONS

As the analysis of the circuits contained in this paper are all made on the Laplace Transform method of linear network analysis, it is assumed that the reader has a working knowledge of this system. Throughout the text, lower case symbols for current (i) and voltage (e) are used to indicate instantaneous values in the time domain. Capital letters (upper case) are used to indicate the values of current (I) and voltage (E) in the frequency domain. In other words,

$$\mathcal{L}\left[f(i)\right] = f(I)$$

$$\mathcal{L}^{-1}\left[f(I)\right] = f(i)$$

The letter (s) is used as the Laplacian operator symbol.

| | |
|---|---|
| PRF | -Pulse Repetition Frequency, cycles per second. |
| $\tau$ | -Pulse Width, seconds, or micro-seconds. |
| AC | -Alternating Current, sine waveform. |
| DC | -Direct Current |
| FM | -Frequency Modulation |
| R - C | -Resistance, ohms - Capacitance, farads |
| L | -Inductance, henries |
| f | -Frequency, cycles per second |
| $\omega$ | -Frequency, radians per second. |
| Q | -Figure of merit for a circuit. $Q = \frac{\omega L}{R}$ |
| $\eta$ | -Efficiency |
| N | -Number of turns in a given winding of a toroid |
| n | -Ratio of primary winding to secondary winding |
| P | -Power, watts |
| A | -Cross sectional area of a toroid, $(cm)^2$ |

| | |
|---|---|
| h | -Height of a toroid, inches. |
| d | -Diameter of a toroid, inches or centimeters. |
| B | -Flux density, gauss per square centimeter. |
| H | -Magnetizing force, oersteds |
| RF | -Radio Frequency, cycles per second |
| cps | -Cycles per second |
| ⍜ | -Source of AC power. |
| k | -Toroidal winding factor |
| K | -Toroidal core factor |
| c.m. | -Circular mils |
| mil | -0.001 inches |
| J | -Joules per cubic centimeter per cycle. |

# CHAPTER I

## INTRODUCTION

Historically, the development of the magnetic modulator started in 1940, when W. S. Melville, [5] B.Sc. (Eng), while testing with pulses some thin strip nickel iron magnetic cores for use in radar pulse transformers, noted the phenomenon as given in Figure 1. This was observed when a one micro-second pulse was applied. The complete reaction took place in about one micro-second. It was noticed that a large and rapid change in impedance occurred at point A. This change in impedance also shows up in the wave form of the current flowing in the winding of the magnetic core. (See Figure 2.) This large change in the incremental permeability of the material took place in approximately 0.1 of a micro-second. This immediately suggested the possibility of utilizing this property for switching high power. As far as can be determined, Melville is the first one to realize the possibility of using this non-linear property of ferro-magnetic material as a basis for high power, high rate switching.

Enough investigation was completed at this time to specify the requirements of the magnetic material in a general way. These requirements are as follows:

1. The material should have a "rectangular" hysteresis loop characteristic.

2. The material used in the cores must preserve these properties when rolled to a thickness of one or two mils. This thickness is required to hold core losses to a minimum.

In 1942, a circuit was built using a combination of a hard tube and

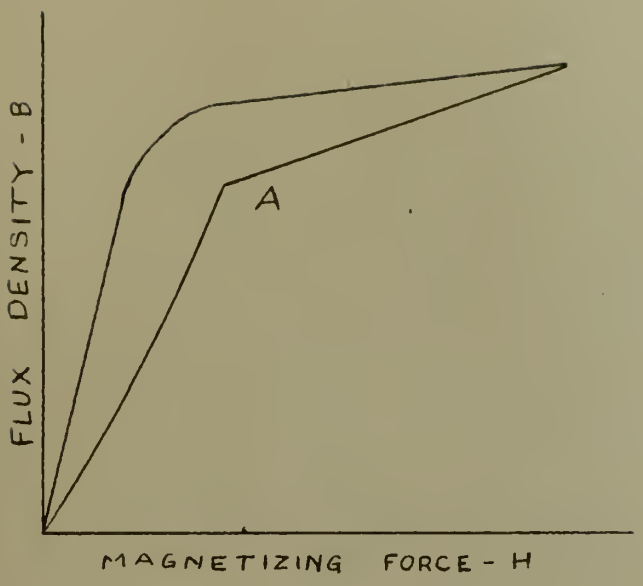


Figure 1. B/H Loop

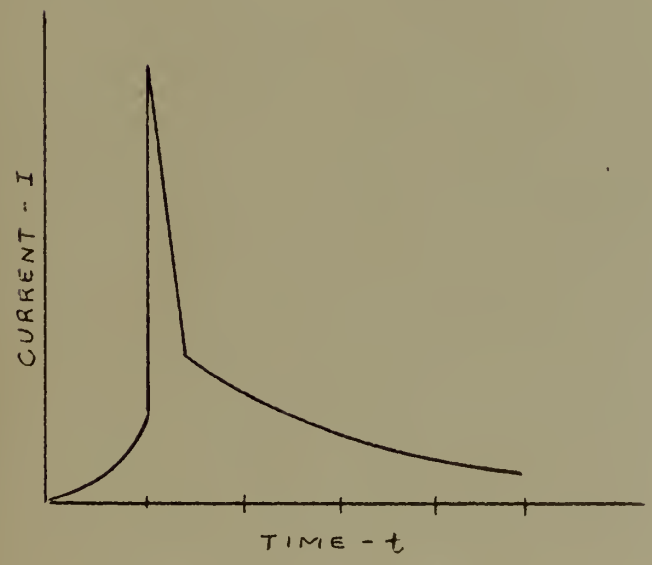


Figure 2. I vs. time

a saturable core. It was successfully utilized in an experimental installation. In 1943, Melville continued on in this field, using a saturable core for switching. Little advancement was made from then on until the year of 1945 when the unidirectional property of the saturable core by current biasing was realized. By properly applying a polarizing bias to the core, pulses which are unidirectional can be produced.

The Germans, in the meantime, developed a magnetic material of properties substantially the same as those required by this circuit. When hostilities ceased in 1945, a British scientific team, while searching records left by the Germans, found the results. In 1948, this material became available in quantity, and further research was carried out in Great Britain by Melville. A laboratory model of a magnetic modulator was successfully operated on a magnetron load during that year. The particular unit was a four stage cascaded arrangement. This system compared favorably with previous modulators of more orthodox type. It was subsequently installed in a maritime radar for the Merchant Marine trade.

Some more of less desultory work was carried on in the United States in subsequent years. Melville, who initiated so much of the original research, lost interest in the further development of saturable cores for this use. It was not until March 1951, when North American Aviation became interested in the possibilities of the magnetic modulator, that further advancement in the field was made. Concurrently, in Scotland, Ferenti, Inc. of Edinburgh carried out some research into this device. In 1953, this company delivered to the RAF a 250 kilowatt peak RF power airborne interceptor radar, utilizing a magnetic modulator.

By August 1951, North American Aviation had a magnetic modulator suc-

cessfully operating into a magnetron load, in an integrated radar set. This unit delivered 225 kilowatts peak RF power, at 0.5 micro-second pulse width, at a PRF of 2000, in the X band frequency range. It subsequently ran an estimated 2000 hours without a failure of any kind in the modulator unit.

At the present time, units have been built up to a power level of 250 kilowatts peak RF output. Other modulator units of similar design to the engineering model mentioned above, have operated for 400 hours without a failure, and are still operating at this writing. These units have met military specifications for shake and vibration tests of electronic equipment. One of the several attractive features of this unit is that a simple, single phase power source is all that is required. However, the frequency of this power source determines the PRF of the radar transmitter. It must be a multiple of either one, two, three or six times the power input frequency.

North American Aviation is currently producing magnetic modulators in small quantities for installation in airborne fire control and search radars. Further research, leading to the improvement and modification, is continually being carried on. For instance, the use of "C" cores to replace toroids is currently being investigated in the hope of reducing weight and cost. As "C" cores are not strain sensitive as the toroids are, they can be fastened directly to some sort of base plate, thus providing good heat transfer to the chassis of the unit. It is hoped that this system will provide better cooling and that the use of oil filled units, as is now necessary with the toroids, can be replaced.

As the recent development of the magnetic modulator has, in general, been of proprietory interest to the companies involved, there has been

little published in technical journals. Most of the research has been based on Melville's paper on the subject, published in 1951. [5]

The advantages and limitations of the magnetic modulator might be summarized as follows:

Advantages:

1. There are no vacuum tubes in the modulator unit.

2. The unit weighes less, compared to conventional units, for any given single pulse width and PRF.

3. The magnetic modulator has inherent reliability.

4. Maintenance is kept at a minimum.

5. The modulator has less volume, higher density, when compared with conventional units.

6. The shelf life is not affected.

7. Single phase AC power is all that is required for a primary power source.

8. Better packaging of the modulator unit is possible.

9. The cost is cheaper compared with conventional modulators.

10. Either a short or an open circuit on the output does not injure the modulator unit, as long as the period of operation under either condition is not excessively long. (In a typical unit, this period of safe operation is not to exceed four hours.) As a result, no fuzes or circuit breakers are required. Interlocks are required for personnel protection only.

Limitations:

1. The output pulse of the magnetic modulator is limited to one pulse width at a fixed PRF for any given unit, unless the problems of multiple, simultaneous, high voltage switching are undertaken. As will be

shown in Chapter III, the pulse width is a function of the values of the components used, and the PRF is a function of the input AC power frequency.

2. It is not readily feasable to FM the PRF to combat counter measures.

3. Toroidal cores must meet stringent requirements.

4. Nickel, a critical material, is necessary in the manufacture of the toroidal cores.

5. The modulator unit is oil filled for proper insulation and cooling.

6. The repair of the modulator unit may only be accomplished on a high echelon. If the units were not oil filled, this limitation would not hold, as the units could be readily repaired in the field. The only requirement would be the logistic facilities for spare parts supply.

7. Production of these units requires more careful control than conventional modulators.

8. Toroidal cores are difficult to securely fasten in place in a given unit. Due to this limitation on the toroids, military specifications of shake and vibration requirements for electronic equipment was barely met in the initial engineering units. Redesign of the securing method has since been accomplished, and this limitation probably no longer exists. It is interesting to note that shock mounts, typical of installation of most electronic equipment, is not required of this unit, but is bolted directly to the aircraft frame.

This paper shows the step by step analysis of the modulator, first, in a qualitative sense only, and secondly, a mathematical treatment of its operation. This is followed by the consideration of various phases of a series RLC circuit that are pertinent to the design of a given unit, and an analysis of an equivalent circuit for a magnetron load is covered.

Other aspects of the problem, such as the characteristics of the

toroidal material are given, as well as several graphs of the characteristics that are useful for design purposes. This is all finally incorporated in a specific design of such a modulator unit, that illustrates the problems involved.

It is the opinion of this writer, that the development of the magnetic modulator constitutes a real step forward toward reaching the ultimate goal of trouble-free operation of a pulsed radar.

## CHAPTER II

## THEORY OF OPERATION

The schematic of a typical magnetic modulator is shown in Figure 3. Note that the circuit is separated into four functional parts.

1. The charging circuit.
2. The intermediate stage.
3. The final stage.
4. The polarizing circuit.

Note that various points on the schematic diagram are lettered. These points will be referred to in the functional description of the unit in the form of subscripts. For instance, $E_{dg}$ is the voltage of point d with respect to g.

Because of the recurrence of the series RLC circuit, as illustrated in Figure 4, this circuit will be considered in detail.

Referring to Figure 4, note that the initial conditions are:

1. A charge exists in $C_1$, of voltage E.
2. The initial current in the coil L, is zero.

Then, using the Laplace Transform method of linear network analysis,

$$I = \frac{E}{L} \frac{1}{\left(s^2 + \frac{R}{L}s + \frac{1}{LC}\right)} \qquad \text{where} \quad \frac{1}{C} = \frac{1}{C_1} + \frac{1}{C_2}$$

Let $\alpha = \frac{R}{2L}$ , $\beta = \pm\sqrt{\frac{R^2}{4L^2} - \frac{1}{LC}}$ , $\frac{R^2}{4L^2} < \frac{1}{LC}$

Then, $$e_c = \frac{E}{LC_2}\left[\frac{1}{\beta_o^2} + \frac{1}{\beta_o \beta}\epsilon^{-\alpha t}\sin(\beta t - \Psi)\right]$$

Where $\beta_o^2 = \alpha^2 + \beta^2$ , $\Psi = \tan^{-1}\frac{\beta}{-\alpha}$

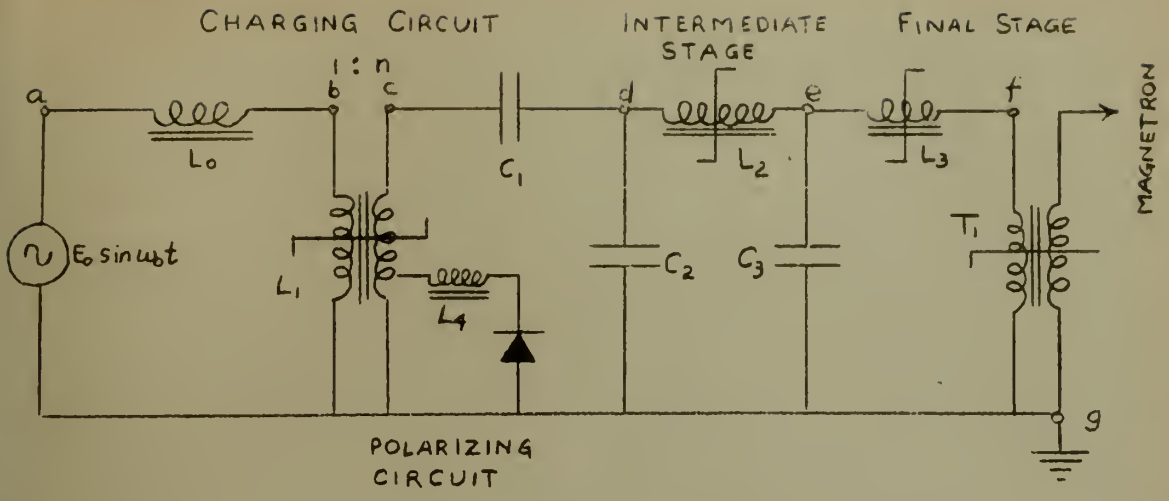


Figure 3. Schematic Diagram of a Typical Magnetic Modulator.

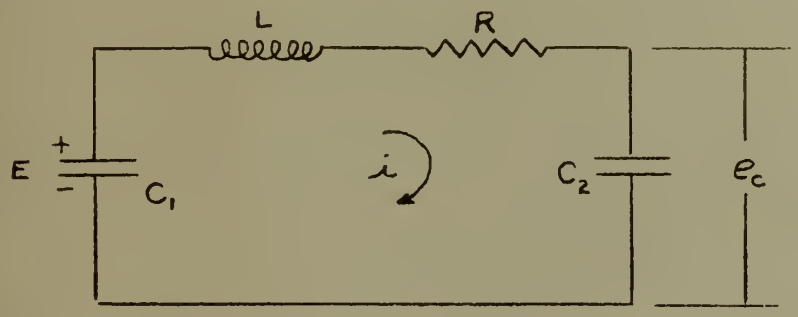


Figure 4. Series RLC Circuit.

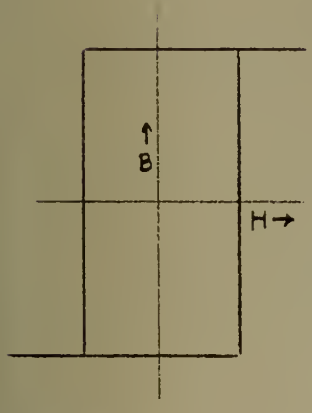


Figure 5. B/H Loop.

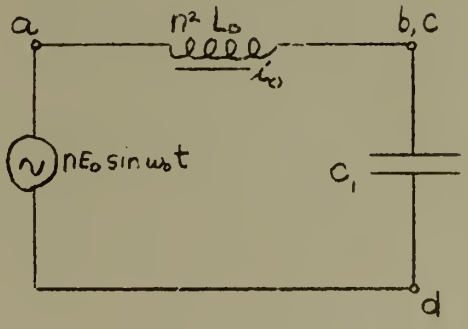


Figure 6. Charging Circuit.

If R is quite small, the output is then the familiar sin wave, with

$$\omega = \frac{1}{\sqrt{LC}} .$$

As a further background, consider a rectangular hysteresis loop, as illustrated in Figure 5. The toroidal reactors, used in the magnetic modulator, use a core whose characteristics closely approach this rectangular B/H loop. When used as a switching device, this component is termed a "pulsactor". The impedance presented to a circuit by such a pulsactor will be quite small when the core is in the saturated condition. On the other hand, when the core is unsaturated, this impedance will be quite high. In this treatment, the pulsactors will be assumed to have the saturated impedance very much less than the unsaturated impedance.

In addition, the saturated inductance of a pulsactor is the same inductance that an air core toroid of the same dimensions and the same number of turns would have. In other words, the saturated inductance is much less than the unsaturated inductance.

Let us now consider the functional description of the charging circuit. As point (d) in Figure 3 is essentially shorted to ground, due to the saturation of $L_2$, $L_3$, and $T_1$, the equivalent circuit as shown in Figure 6 may be drawn. This circuit is basically a series resonant charging phenomenon, with resonance occurring at the input frequency, $\omega_o$.

At $t = 0$, $C_1$ charge = 0, $i_o = 0$. As the circuit is assumed to be lossless, the peak of the voltage across $C_1$, $V_{cd}$, for one cycle charging occurs at $\omega_o t = 2\pi$ and is equal to $\pi n E_o$. Also, the voltage across $C_1$ is across $L_1$. See Figure 7.

The polarizing circuit consists of a rectifier and choke $L_4$ in series with a tapped portion of the secondary of $L_1$. (See Figure 3.) During the

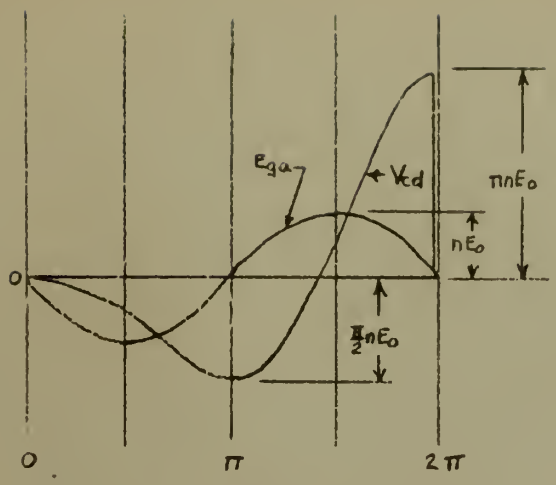


Figure 7. Voltage Waveforms in the Charging Circuit.

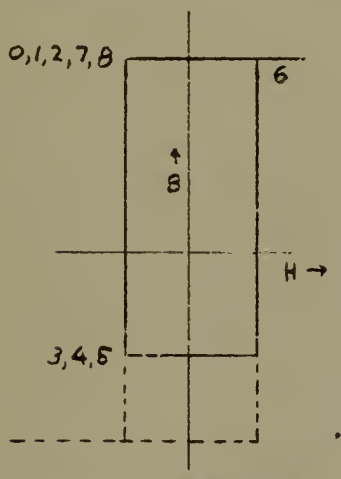


Figure 8. Hysteresis Loop.

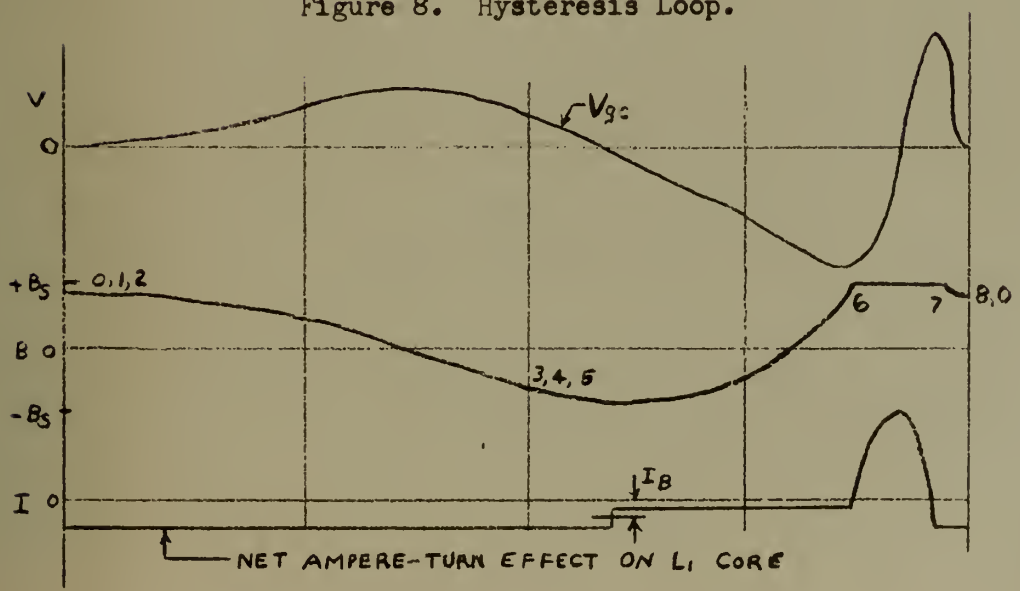


Figure 9. First Stage Wave Forms.

charging cycle, a tapped portion of the secondary winding supplies the voltage $V_{hg}$, which is in phase with and proportional to the total voltage across the secondary winding $V_{gc}$.

The current $i_B$ resulting from the $V_{hg}$ applied to the polarizing circuit is unidirectional due to the presence of the rectifier, and results in an average current $I_B$. (See Figure 9.) This average current produces a positive polarizing magneto-motive force on $L_1$, which makes possible saturation of the $L_1$ core in the positive direction only. This is known as "single cycle firing".

The next step is to functionally describe the intermediate stages. It must be understood that the flux density in the pulsactor, $L_1$, is proportional to the negative voltage-time integral of the voltage across $L_1$. Without the polarizing field, the $L_1$ core would saturate in both the positive and negative directions. Note the dotted portion of the hysteresis loop in Figure 8. However, with the polarizing field, single cycle firing results.

A step by step path around the hysteresis loop during the charging cycle is described by the numbered points, in Figures 8 and 9. The curves start at point (0), which is the end of the pulse out of the final stage. Starting at point (0) on the flux density plot of Figure 9, and proceeding in numerical sequence to the right, the hysteresis loop is traversed to point (6), where $L_1$ saturates and the charge on $C_1$ is transferred to $C_2$. The time required for this transfer from point (6) to point (7) on the curves is determined by the resonant frequency of $C_1$, $L_1$ (saturated), and $C_2$. (See Figure 4, and the accompanying text for this explanation.) The equivalent circuit for this transfer of energy is given in Figure 10, as

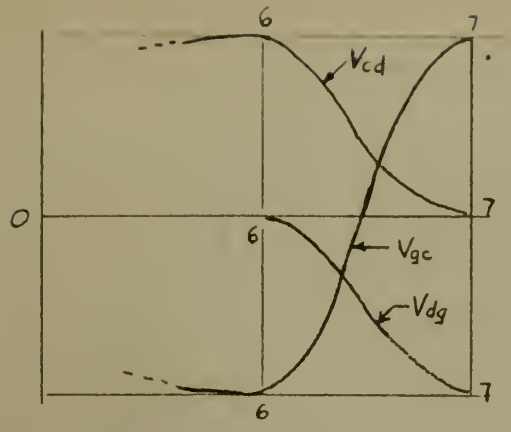


Figure 10. Waveforms of First Stage Pulsactor.

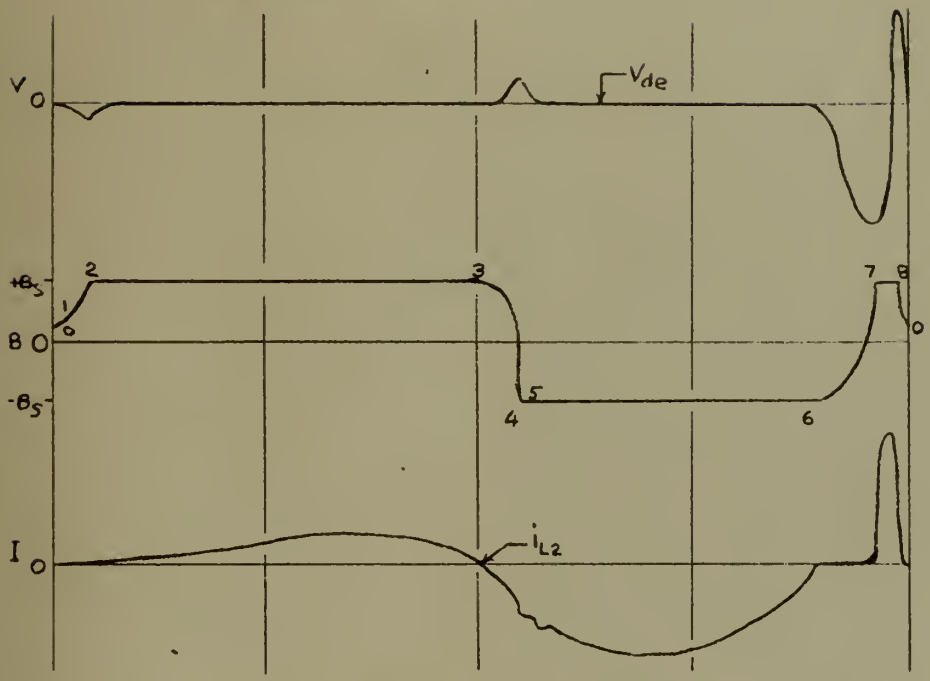


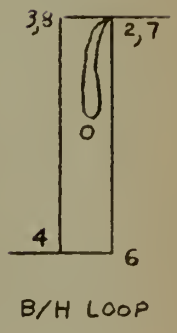


Figure 11. Wave Forms of the Second Stage Pulsactor $L_2$.

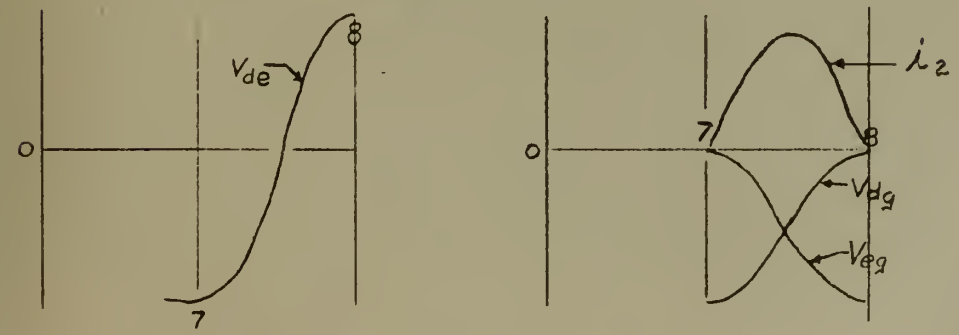


Figure 12. Second Stage Wave Forms.

well as voltage and current waveforms. As $C_1$ discharges, the voltage $V_{gc}$ across $L_1$ goes from negative to positive. This occurs because at point (6) the voltage across $C_1$ is across $L_1$, $C_2$ having no charge. After the discharge of $C_1$ and the charge of $C_2$, at point (7), the voltage impressed across $L_1$ is of the opposite polarity, as may be seen in Figure 10, where the time from (6) to (7) has been expanded. The remainder of the time from point (7) to (0) on the flux density curve of Figure 9 is the time required by $C_2$ and $C_3$ to discharge, as is explained later.

The operation of the second stage can be explained by referring to Figure 11 and Figure 12. The flux density plot starts at point (0), which corresponds to the end of the pulse out of the final stage. Starting at point (0), it is noted that the flux is positive but is less than $+B_s$. At the start of the charging cycle, the voltage $V_{cg}$ is of the polarity to cause pulsactor $L_2$ to go into saturation in the positive direction in a very short time. Saturation occurs at point (2), and $L_2$ remains in saturation until point (3). At this point the current has reversed direction, the voltage drop across $L_2$ is in the direction opposite to that causing saturation, and $L_2$ is brought out of saturation. The hysteresis loop is traversed to point (4), at which time $L_2$ goes into saturation in the negative direction and stays in saturation to point (6). It is at this time that $L_1$ saturates and the voltage across $C_2$ begins to build up. The voltage build-up across $C_2$ is opposite in polarity to the voltage that caused $L_2$ to saturate at point (4). Hence, $L_2$ comes out of saturation at point (6) and the hysteresis loop is traversed to point (7), at which time the energy has all been transferred from $C_1$ to $C_2$. At point (7), $L_2$ saturates and the

charge on $C_2$ is transferred to $C_3$. The time required for the transfer from point (7) to point (8) is determined by the resonant frequency of $C_2$, $L_2$, (saturated), and $C_3$.

It will be noted in the expanded curves in Figure 12 that as $C_2$ discharges, the voltage $V_{de}$ across $L_2$ goes from negative to positive during saturation. This occurs because at point (7), $C_2$ is charged, $C_3$ has no charge, and the voltage across $C_2$ is across $L_2$. After $C_2$ is discharged and the voltage across $C_3$ rises to that shown at point (8), the voltage impressed on $L_2$ is of the opposite polarity, as "d" is essentially at ground at point (8). The discharge current in the second stage is shown as $i_2$ in Figure 12.

The remainder of the time on the flux density curve (Figure 11), from point (8) to point (0), is the time required for the final stage to discharge $C_3$. $L_2$ comes out of saturation and the loop within the hysteresis loop is traced from (8) to (0). At this point one cycle in the second stage is complete.

In the final stage, the analysis differs from the previous stages, in that the energy is dissipated in a load, when the capacitor discharges, instead of transferring to another capacitor. To explain the operation of the final stage, Figures 14, 15, and 16 will be referred to. As in the previous figures, point (0) in Figure 14 corresponds to the end of the pulse out of the final stage. Starting at this point, $L_3$ is in saturation in the positive direction. Thus, the first half of the charging cycle holds it in saturation. In Figure 15, at point (0), the flux in the pulse transformer $T_1$ is just short of saturation in the positive direction. The voltage at the first of the charging cycle is of the polarity to cause

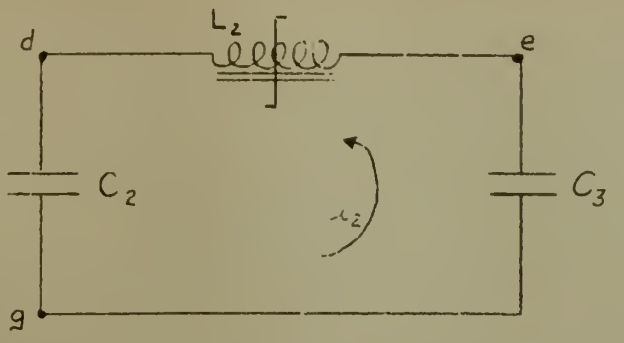


Figure 13. Schematic of Second Stage.

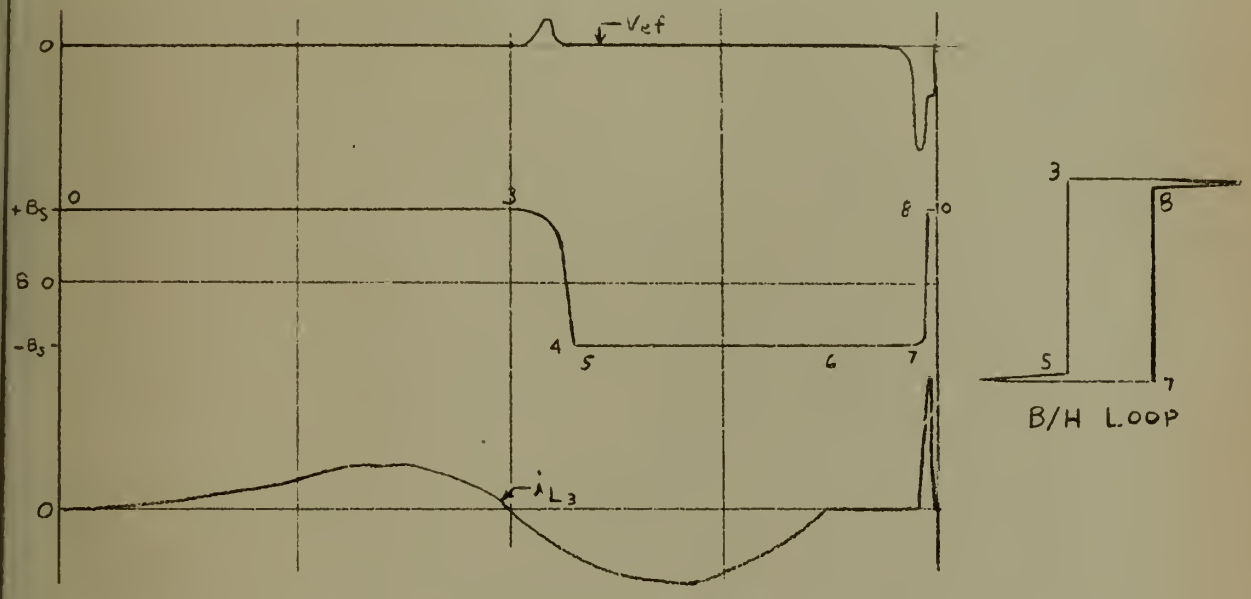


Figure 14. Wave Forms of Third Stage Pulsactor, $L_3$.

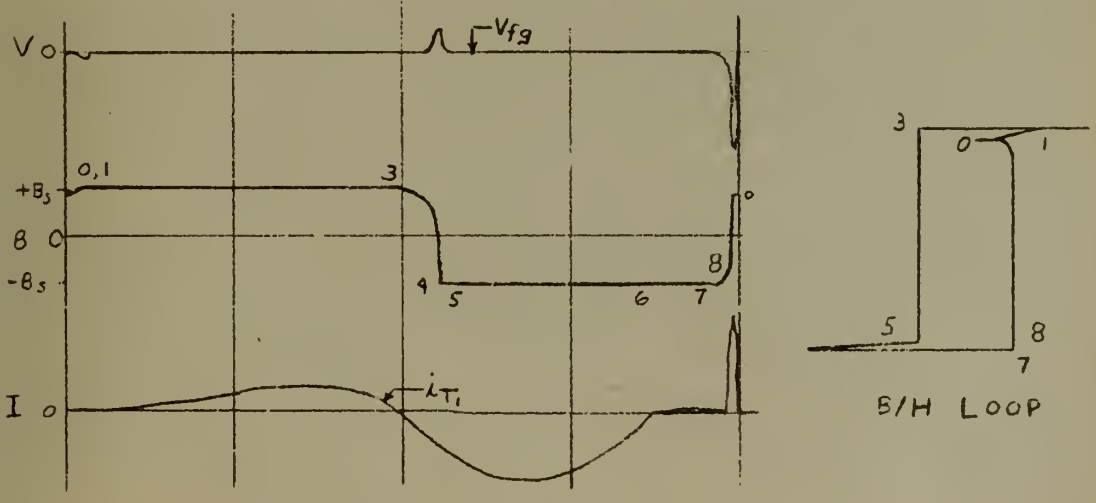


Figure 15. Wave Forms of Pulse Transformer $T_1$.

$T_1$ to saturate in the positive direction, which it does in a very short time after the start of the cycle, as shown by point (1). Both $L_3$ and $T_1$ stay in saturation until point (3). At this point the charging current has reversed polarity and both $L_3$ and $T_1$ come out of saturation.

From the previous discussion it will be noted that $L_2$ also comes out of saturation at point (3). The impedance of $L_2$ is many times that of $L_3$, and likewise, the impedance of $L_3$ is much greater than that of $T_1$. Remembering that the flux density is proportional to the negative voltage-time integral of the voltage wave, it will be seen that with $L_2$, $L_3$, and $T_1$ in series following point (3), the greatest voltage drop will be across $L_2$. Hence, $L_2$ will go into saturation first, then the greatest voltage drop will be across $L_3$, causing it to go into saturation next, followed closely by $T_1$. In Figure 14 and 15, $L_3$ and $T_1$ are shown to saturate in the negative direction at point (5). $L_3$ and $T_1$ remain in saturation to point (7). At this time $L_2$ has saturated and $C_3$ begins to charge. This can be seen by referring to Figure 16. It is seen that the voltage across the capacitor $V_{eg}$ builds up to point (8). As the voltage builds up across $C_3$, the major part of the voltage is impressed on $L_3$ because its impedance is many times greater than that of $T_1$. During this interval, the impedance of $T_1$ is essentially a magnetizing reactance because the non-oscillating magnetron provides an open circuit across the secondary. This equivalent circuit is shown in Figure 16, with switches $S_1$ and $S_2$ open. $L_3$ saturates at point (8), causing most of the voltage to be impressed on $T_1$. This is simulated by closing switch $S_1$.

The voltage across $T_1$ increases until the magnetron oscillates, at

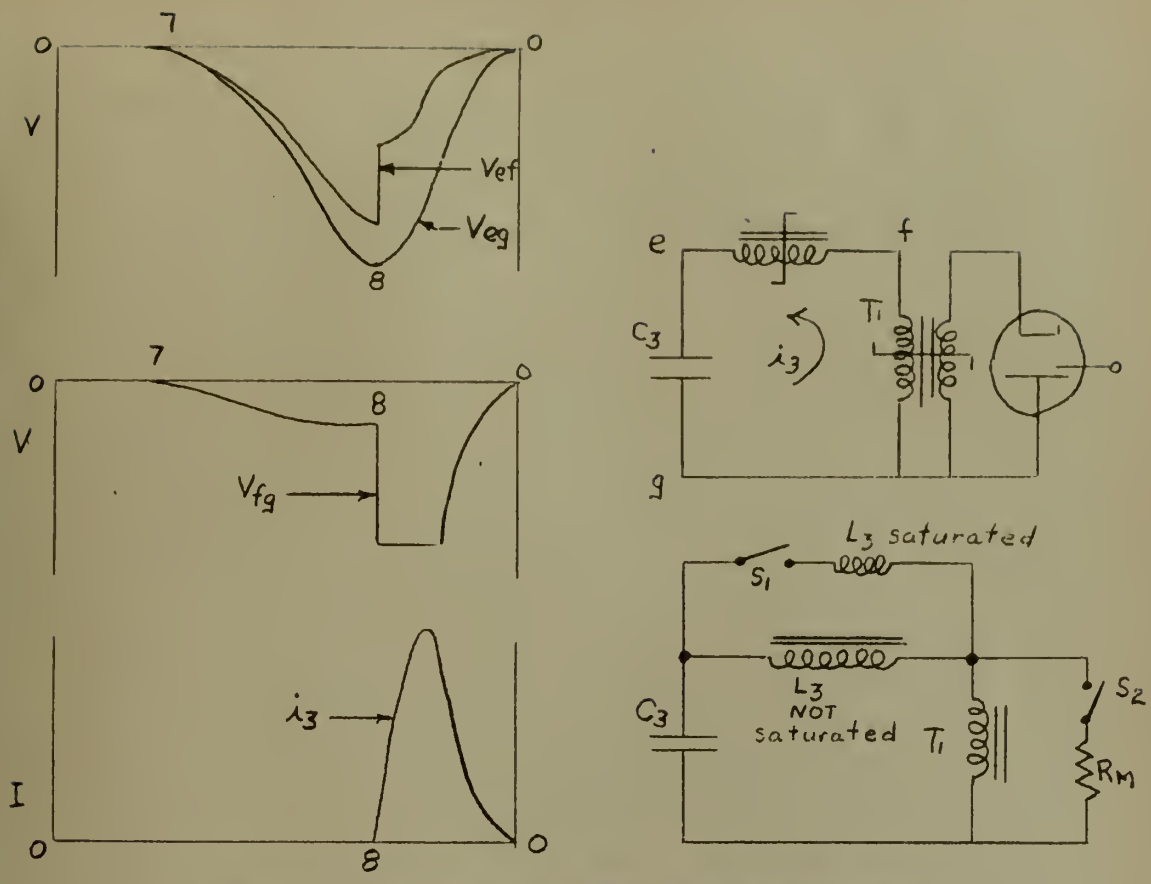


Figure 16. Third Stage Schematic and Wave Forms.

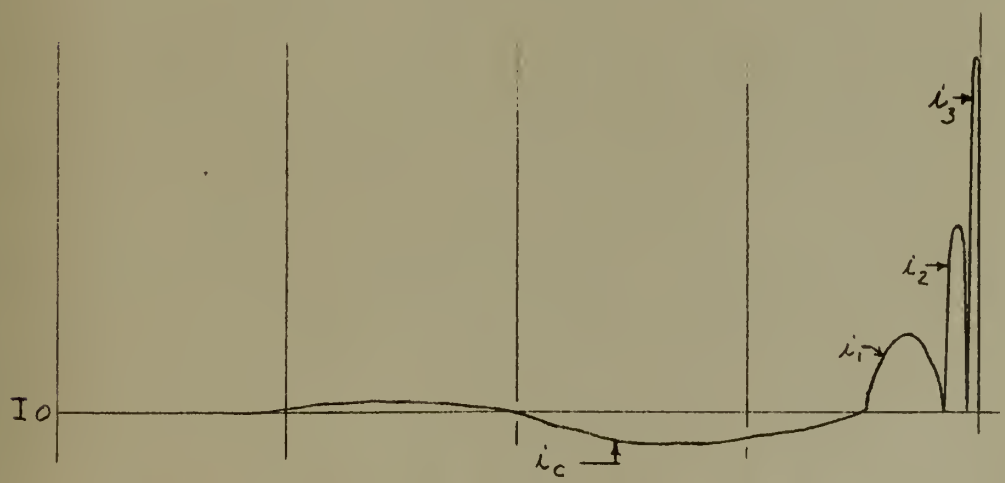


Figure 17. Current Amplitudes and Time Positions.

at which time the magnetron impedance decreases to a dynamic resistance that is a function of the magnetron being used. This is simulated by closing switch $S_2$. As the magnetron is a voltage regulator while oscillating, the voltage across $T_1$ is held constant until the magnetron drops out of oscillation. The equivalent circuit with both switches closed is a critically damped RLC series circuit.

At point (0) the energy stored in $C_3$ has been dissipated in the magnetron and one cycle has been completed. The voltage-time area is not great enough to cause $T_1$ to saturate in the discharge time from points (8) to (0) in Figure 15. Hence, the flux is just short of saturation at the beginning of the cycle.

The saturated inductance of the pulsactors is much less than the unsaturated inductance. The sudden decrease of inductance upon saturation results in a discharge frequency higher than the charging frequency. As a result, with each transfer of energy, the pulse width is narrowed and the specified pulse width is obtained in the final stage. Figure 17 shows the decrease in current pulse width as the energy is transferred from one stage to the next.

Observed pulse to pulse jitter, (in this case, jitter is the consistency of the firing point on the time scale) of a similar radar modulator to the one just described in this text, as observed by Melville, [5] was better than 0.005 micro-seconds between output pulse and the discharge of the first stage. When the unit fires will depend upon the frequency stability of the power supply. It has been found in practice that a variation of $\pm$ 5% in the input frequency has little effect on the power output, and no effect on the pulse width. For example, on a particular unit

designed to operate on an input frequency of 350 cps, the frequency was varied from 290 cps to 450 cps. The peak power output varied from 196 kilowatts, to 143 kilowatts. This was a variation around the design output of +11% to -19%. The pulse width remained constant. The overall efficiency on this unit ran from 25% to 30%. It is readily seen that the regulation on a standard alternator would be well within the tolerance of the modulator.

# CHAPTER III

## ANALYTIC TREATMENT OF THE MAGNETIC MODULATOR

A rigid mathematical analysis of the magnetic modulator has never been made. Its non-linearity of operation has prevented this. However, by making certain assumptions, and using linear methods of analysis, an approach that has proven quite satisfactory for toroidal cores can be attacked.

In the mathematical analysis, the equations that are useful in the actual design, or the derivations that will be referred to later on in the text, are all numbered. The Laplace transform pairs that are derived in the frequency domain, and then transferred to the time domain, are followed by a number in a parenthesis, as .....(2.511). This number is the transform pair used, as listed in the appendix of transform pairs in Gardner and Barnes. [1]

The following assumptions are made in the approach to the design criteria:

1. All elements are lossless.

2. There is equal frequency multiplication from stage to stage. The phenomenon of the pulse width narrowing from stage to stage, as the cores saturate, is referred to as "frequency multiplication".

3. The same energy (volt-seconds) is stored in each C.

4. All C's are to be equal.

5. The load presented by the magnetron is a constant R.

6. When saturated, the pulsactors appear as an air core toroid. See page 10.

The following requirements are assumed known:

1. $P_{MAG}$ - Magnetron peak power out (RF Peak Power).

2. $f_o$ - Input frequency from the power supply. This is a fixed frequency.

3. $\tau$ - Pulse duration, as measured between the $\frac{1}{2}$ power points of the output.

4. $\eta$ - Estimate of the efficiency.

5. The Characteristic curves of the magnetron.

It is now necessary for the engineer to determine:

1. C.

2. $v_1$, $v_2$, $v_3$, the voltages across $C_1$, $C_2$, $C_3$.

3. The saturated L of each core.

4. The number of turns, N, and the cross sectional area, A, of each pulsactor.

5. The design of the pulse transformer.

The basic schematic, with the symbols as used throughout the rest of this treatment, is given in Figure 18.

The energy stored in a capacitor is $\frac{Cv^2}{2}$. The energy in the output of the magnetron is $P\tau$. The unit is considered lossless, hence, $\frac{Cv^2}{2} = P\tau$. v is selected in consideration of the value of $n_2$ (4 to 10 usually), and keeping v low enough to avoid corona effects, but high enough to avoid large values of current, and hence large wire size. Taking the above into consideration, v is then selected.

Then, $C = \frac{2P\tau}{v^2}$ .....I

Considering the junction between $C_1$ and $C_2$ as shorted to ground, due to the saturation of $L_2$, $L_3$, and $T_1$, the circuit is as given in Figure 19. A further simplification of the basic circuit is made at this point to

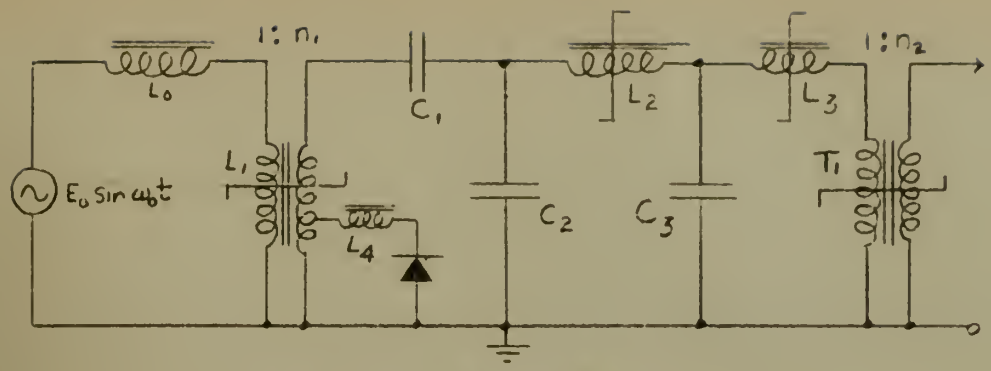


Figure 18. Basic Schematic.

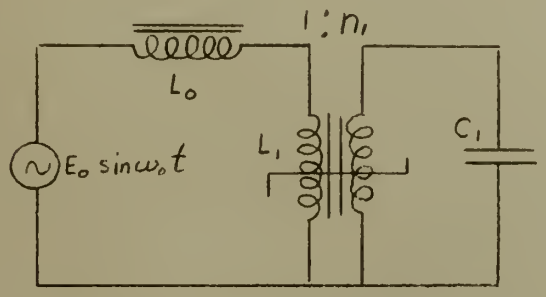


Figure 19. First Stage Schematic.

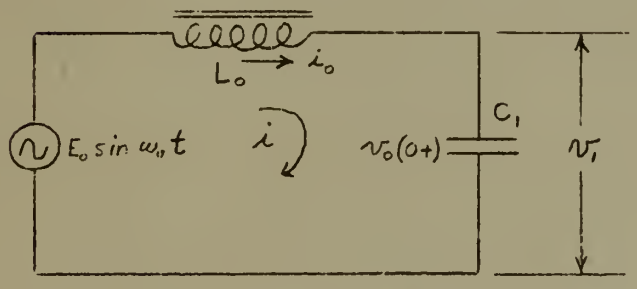


Figure 20. Simplified First Stage Schematic.

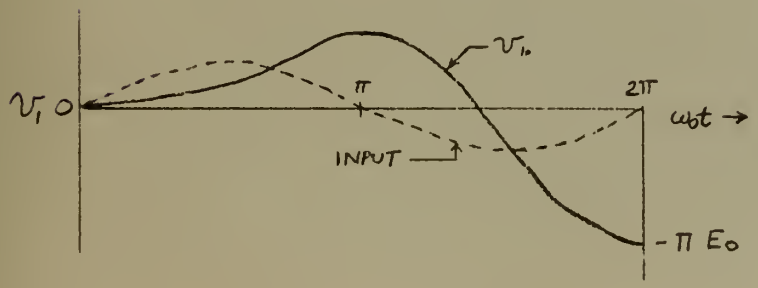


Figure 21. Plot of $v_1$ vs. $\omega_0 t$ .

simplify the problem further. The transformer, $L_1$ is considered ideal, and the circuit as given in Figure 20 results. The effect of the transformer will be reintroduced into the problem further on in this chapter.

The initial conditions of the circuit as given in Figure 20 are:

$$i_o = 0 \quad , \quad v_o(o+) = 0 \quad , \quad \omega_o^2 = \frac{1}{L_o C_1} .$$

Then, proceeding around the circuit in a clockwise direction, as indicated in Figure 20,

$$\frac{L_o}{s}\left[s^2 + \frac{1}{L_o C_1}\right] I = E_o\left[\frac{\omega_o}{s^2 + \omega_o^2}\right]$$

As $$V_1 = \frac{I}{C_1 s} = E_o \omega_o^3 \frac{1}{(s^2 + \omega_o^2)^2}$$

Then, $v_1 = \frac{1}{2} E_o (\sin \omega_o t - \omega_o t \cos \omega_o t)$ .....(2.501) II

$v_1$ maximum occurs, for single cycle operation, at $t = \frac{2\pi}{\omega_o}$ . This value is $v_1 = -\pi E_o$. For the plot of $v_1$ vs. $\omega_o t$, see Figure 21.

As the power source is considered to have zero impedance, the voltage across $C_1$ at time $t = \frac{2\pi}{\omega_o}$ is also across $L_o$. Now, $-\int v_1 \, dt = N_1 \phi$, where $\phi$ is the total flux per turn in the core of the pulsactor, and $N_1$ is the number of turns of wire around it. By inserting equation II in the above expression, the following derivation is obtained:

$$\int v_1 \, dt = E_o\left[\frac{1 - \cos \omega_o t}{\omega_o} - \frac{t}{2} \sin \omega_o t\right] = -N_1 \phi \text{ ..... III}$$

This same $v_1$ will be present in our ideal transformer, $L_1$. It is desired to have $L_1$ stay in the unsaturated condition and therefore act as a transformer until $\omega_o t = 2\pi$ is almost reached. At that time, $L_1$ becomes saturated due to the action of $L_2$, $L_3$, and $T_1$ as explained in Chapter II. Referring to the equation, $-\int v_1 \, dt = N_1 \phi$, it is apparent that $\phi$ maximum occurs when $v_1$ is passing through zero during its one cycle excursion.

This then constitutes the limiting condition that the pulsactor $L_1$ goes through without saturation. To determine what $N_1\phi$ will be required to allow $L_1$ to be just short of saturation, it becomes necessary to solve for $\omega_o t$ in equation II when $v_1 = 0$. By then substituting this value of $\omega_o t$ in equation III, the $N_1\phi$ may be determined.

Now solve for $\omega_o t$ in the expression $\sin \omega_o t = \omega_o t \cos \omega_o t$. This occurs when $\omega_o t = 4.493$ radians. ($258^\circ$)

Evaluating equation III at this value of $\omega_o t$, $N_1\phi$ is found to be

$$N_1\phi = \frac{E_o}{f_o} \frac{3.4}{2\pi} \qquad \text{.....IV}$$

But $N_1\phi = N_1 \Delta\beta A_1 \times 10^{-8}$ , where $\Delta\beta$ is defined in Figure 22, and $A_1$ is the cross sectional area of the $L_1$ core, in square centimeters.

From Figure 22, $\phi = 2 \beta_{MAX} A_1 \times 10^{-8}$

Therefore, $N_1\phi = 2N_1 \beta_{MAX} A_1 \times 10^{-8}$

Therefore, $N_1A_1 = \left[\frac{E_o}{\beta_{MAX} f_o}\right] \frac{3.4}{4\pi} 10^8$ ---------- V

where the units are,

$A_1$ - square centimeters.

$\beta_{MAX}$ - gauss/ $cm^2$

$E_o$ - volts.

$f_o$ - cps.

$\beta_{MAX}$ is selected on the basis of the characteristics of the core that is used. All other factors are known, therefore, the quantity $N_1A_1$ is uniquely determined.

Since a pulsactor in a saturated condition can be considered to be an air core toroid, the equation for such a configuration, as given in Terman's "Radio Engineer's Handbook" [6] can be used. This equation is:

$$L_{1s} = (0.0117)\ 10^{-6}\ N^2\ h \log_{10}\left(\frac{d_2}{d_1}\right) \text{ henries.} \quad \text{. . VI,}$$

where $L_{1s}$

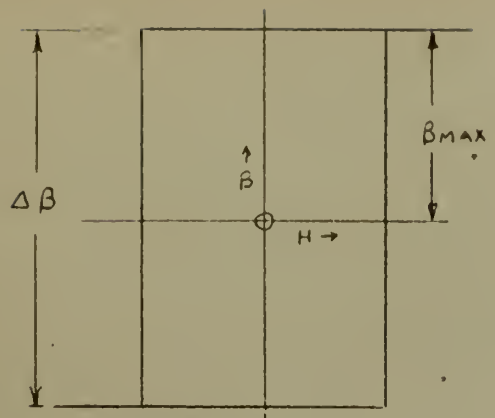


Figure 22.
B/H Loop of the $L_1$ Core.

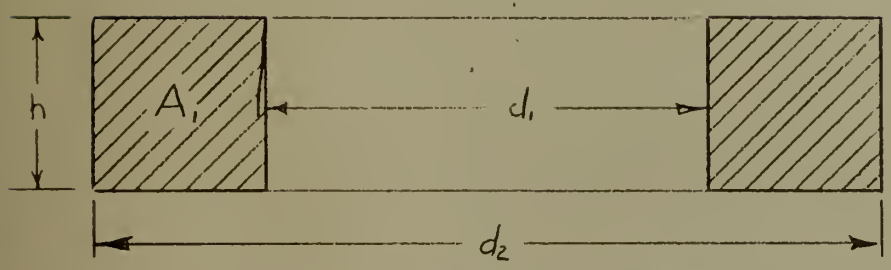


Figure 23. Cross Section of Pulsactor $L_1$.

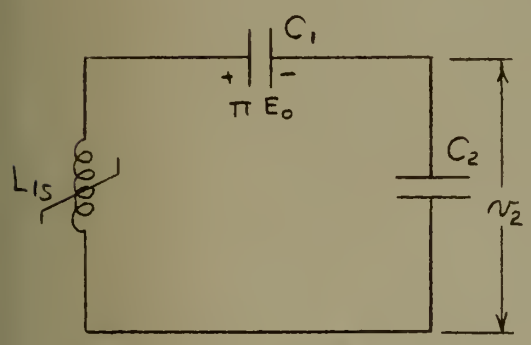


Figure 24. First Stage.

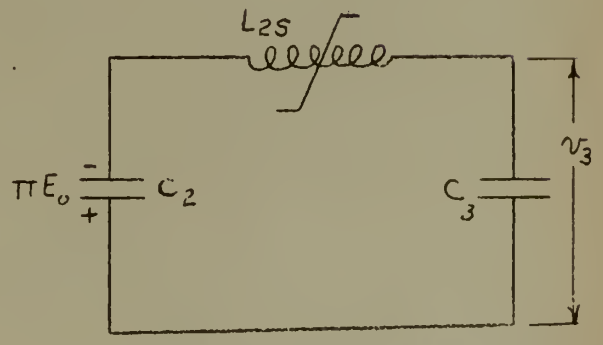


Figure 25. Equivalent Circuit of Second Stage.

is the saturated inductance of pulsactor $L_1$,

h is the height of the toroid, in inches,

$d_2$ is the outside diameter of the core,

$d_1$ is the inside diameter, and

N is the number of turns of wire around the core.

Assuming the core to have a rectangular cross section, as illustrated in the sketch in Figure 23, $h = \frac{2A_1}{d_2 - d_1}$.

Then, $L_{1s} = N_1^2 A_1 \left(\frac{.0234}{d_2 - d_1}\right) 10^{-6} \log_{10} \frac{d_2}{d_1}$.

Under the assumption of equal frequency multiplication for each stage, and using three stages, as illustrated in Figure 18, $f_1 = \sqrt[3]{\frac{f_{out}}{f_o}} \times f_o$ where $f_1$ is the frequency of the first stage. Then, by defining $f_{out} = \frac{1}{2T}$

$$f_1 = \sqrt[3]{\frac{1}{f_o 2T}} \times f_o \qquad \text{.....VII}$$

The discharge circuit of $C_1$ is shown in Figure 24. From this, the natural "ringing" frequency of the circuit is,

$$f_1 = \frac{1}{2\pi\sqrt{L_{1s}\frac{C_1}{2}}} \qquad (\text{as } C_1 = C_2).$$

Therefore, $L_{1s} = \frac{1}{2\pi^2 f_1^2 C_1}$ .....VIII

By substituting the above in equation VI, you arrive at the following equation. $N_1^2 A_1 = \frac{(d_2 - d_1)10^6}{2\pi^2 f_1^2 C_1 (.0234) \log_{10} \frac{d_2}{d_1}}$ .....IX

Using equations V and IX, the $N_1$ and $A_1$ of the first pulsactor, $L_1$ are now determined.

In considering the second stage, an appreciation of the time axis must be had or the steps are not readily apparent. $L_2$, $L_3$, and $T_1$ are now in the unsaturated condition, so their high impedance essentially opens the circuit between the top of $C_2$ and ground. The energy is then transferred from $C_1$ to $C_2$ through $L_{1s}$, at a frequency $f_1$. The equation of the

voltage across the capacitor $C_2$ is then $v_2 = -\frac{\pi E_o}{2}\left[1 - \cos \omega_1 t\right]$.

Using the method of analysis as illustrated in deriving the first stage, it is found that

$$2 B_{max} N_2 A_2 \times 10^{-8} = \int_o^{T_1} v_2 \, dt = \frac{\pi E_o}{2}\left[t - \frac{1}{\omega_1} \sin \omega_1 t\right]_o^{T_1}$$

Evaluating the above between the limits indicated,

$$N_2 A_2 = \frac{\pi E_o}{2} \frac{1}{4 B_{max} f_1} \times 10^8 \qquad \text{.....X}$$

Due to the assumption of equal frequency multiplication per stage, $f_2 = \left(\frac{1}{f_o 2 \tau}\right)^{2/3} \times f_o$.

As $L_1$ and $L_3$ are now in an unsaturated condition, and present a high impedance, the equivalent circuit is as shown in Figure 25. Then,

$$f_2 = \frac{1}{2\pi \sqrt{L_{2s} C_2/2}} \qquad \text{or } L_{2s} = \frac{1}{2\pi^2 f_2^2 C_2} \qquad \text{.....XI}$$

From the results of equation XI, and substituting in equation VI,

$$N_2^2 A_2 = \frac{(d_2 - d_1) 10^6}{2\pi^2 f_2^2 C_2 (.0234) \log_{10} \frac{d_2}{d_1}} \qquad \text{.....XII}$$

By using equations X and XII, the $N_2$ and $A_2$ of the second pulsactor, $L_2$ are uniquely determined.

By referring to Figure 25, the voltage across $C_3$ may then be written as $v_3 = \frac{\pi E_o}{2}(1 - \cos \omega_2 t)$.

In the design of the third stage, certain assumptions must be made to arrive at some design criteria. These assumptions are:

1. An ideal pulse transformer, $T_1$ is assumed.

2. $\tau$ is the time between the $\frac{1}{2}$ power points of the RF envelope. See Figure 26.

3. The load is a resistance of such a value that the circuit is a critically damped series RLC circuit.

Under assumption 2, the time $\tau$ is also assumed to be the time between

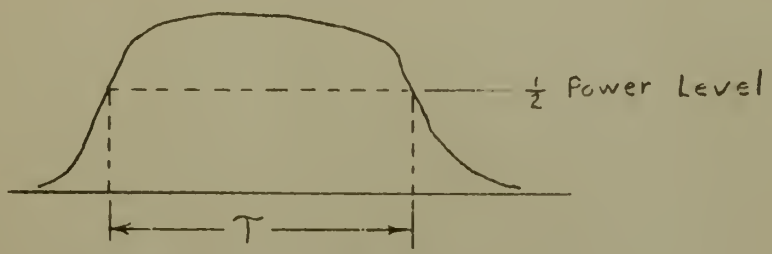


Figure 26. RF Envelope.

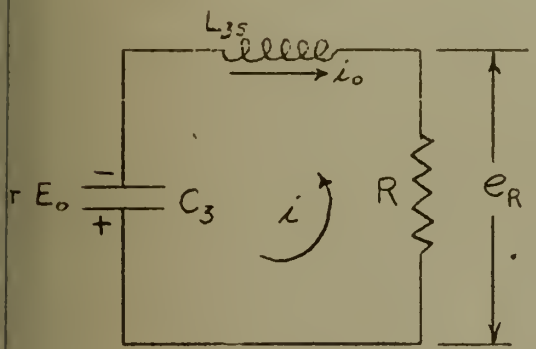


Figure 27.
Final Stage Schematic.

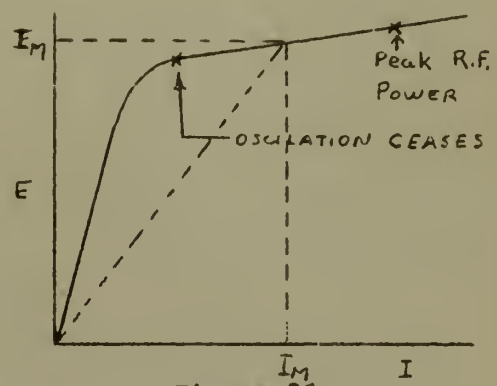


Figure 28.
Characteristic Curve of a Magnetron, Showing where $R_{mag}$ is measured.

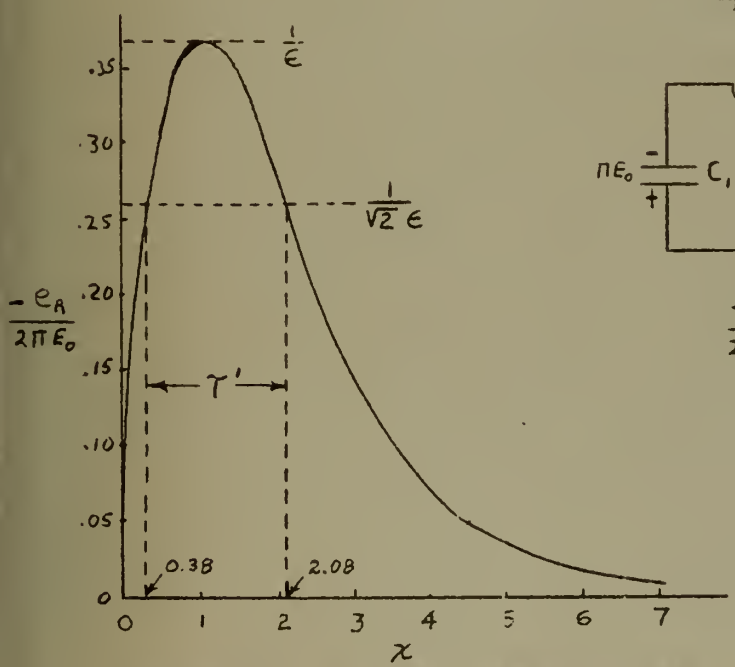


Figure 29. Voltage Waveform Across the Resistance R, in a Critically Damped Series RLC Circuit.

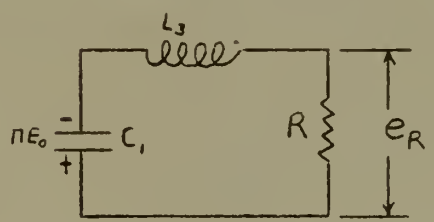


$$\frac{-e_R}{2\pi E_o} = \chi \epsilon^{-\chi}$$

where $\chi = \frac{R}{2L_3}$

the ½ power points of the voltage wave form across the resistance of a critically damped series RLC circuit. This waveform is plotted in Figure 29. It is true that the magnetron load is far from a pure resistance, but for design purposes, this has proven to be adequate. For further justification, see the development in Appendix A. It has been experimentally determined that $\tau$ is approximately half the period of an undamped sin wave of the final LC circuit.

In consideration of these assumptions, and letting $T_1$ be an ideal pulse transformer, the circuit may be represented as shown in Figure 27. Here, $R = \frac{R_{MAG}}{n_1^2}$, and $R_{mag}$ is the geometric mean of the resistance of the magnetron at peak power conditions, and the resistance of the magnetron where oscillation ceases. This is displayed pictorially in Figure 28, the characteristic curve of a magnetron.

From Figure 28, $R_{mag} = \frac{E_M}{I_M}$ .....XIII

The initial conditions are $i_o = 0$, and the charge on $C_3$ results in a voltage stored in it of $\pi E_o$. For critical dampening, $R = 2\sqrt{\frac{L_3}{C_3}}$ . This then results in the familiar result of

$$i = -\frac{\pi E_o}{L_3} t \, \epsilon^{\frac{-Rt}{2L_3}}$$

Then, $e_R = -\pi E_o \frac{R}{L_3} t \, \epsilon^{\frac{-Rt}{2L_3}}$ .....XIV

It is further noted that $e_R \text{ max} = \frac{2}{\epsilon}(-\pi E_o)$ and occurs at $t = \frac{2L_3}{R}$ . The half power points occur when $e_R = \frac{e_{R\,MAX}}{\sqrt{2}}$ . By letting $x = \frac{R}{2L_3} t$ , the equation for $e_R$ can be written as follows:

$$e_R = (-2\pi E_o) x \, \epsilon^{-x}$$ .....XV

By letting equation XV equal its value at the half power points, namely, $\frac{\sqrt{2}}{\epsilon}(-\pi E_o)$ , it is now possible to solve for the values of x at which

this occurs. This results in

$x_1 = 0.38$

$x_2 = 2.08$

Therefore, $\frac{R}{2L_3}(\tau) = 1.70$, or $\tau = 3.40\,\frac{L_3}{R}$ .....XVI

Remembering, that for critical dampening, $R = 2\sqrt{\frac{L_3}{C_1}}$ , you now have uniquely determined the two unknowns $L_3$ and R, by the utilization of this criteria, and equation XVI.

As, $n_2^2 = \frac{R_{mag}}{R}$ , you have now also determined the step up ratio, $n_2$ of the pulse transformer, $T_1$.

The actual voltage waveform in a critically damped series RLC circuit is shown in Figure 29. For convenience in plotting, a normalized plot is used, and the actual equation plotted is $\frac{-e_R}{2\pi E_o} = \lambda \epsilon^{-\lambda}$. Note that the rise time is rapid.

The effect of $n_1$, the voltage step up ratio in the first transformer, $L_1$ is given below. The equivalent circuit to be studied is shown in Figure 30. $L_1$ is assumed to be an ideal transformer. Note that for resonance charging, $\omega_o = \frac{1}{\sqrt{L_o C_1 n_1^2}}$ .

Then, $L_o = \frac{1}{\omega_o^2 C_1 n_1^2}$ .

The voltage across the condenser, $C_1$ is noted to be,

$$v_1 = \frac{1}{2} n_1 E_o (\sin \omega_o t - \omega_o t \cos \omega_o t)$$

Solving for what this voltage will be at the end of one cycle of charging, $v_1$ max. $= -\pi n_1 E_o$.

Therefore, for all previous derivations, it is now possible to insert $(-\pi n_1 E_o)$ wherever the expression $(-\pi E_o)$ has occurred. The derivations will then be correct for the circuit as shown in Figure 18.

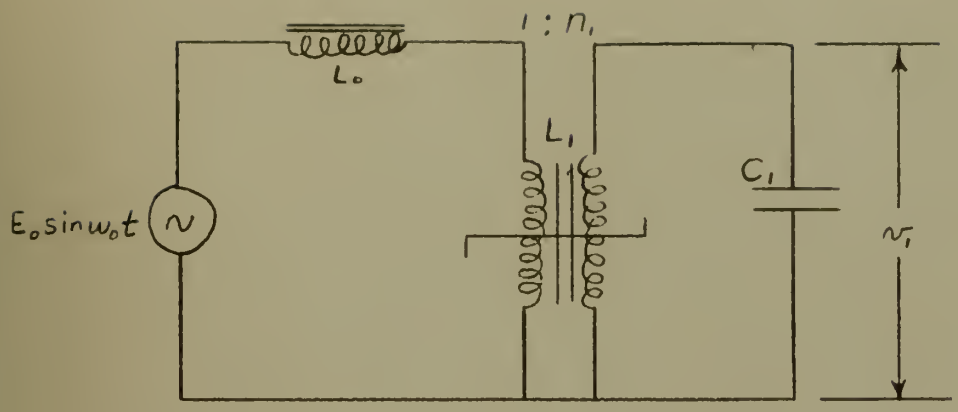


Figure 30. Schematic Diagram of the First Stage, Including the Step-up Transformer $L_1$.

# CHAPTER IV

## CIRCUITS WITH LOSSES

This treatment of the analysis of a magnetic modulator has so far assumed all the circuits to be lossless. This is, of course, far from the truth. Every time some component is inserted into a circuit, there exists losses of one kind or another. In this unit, the main source of power loss lies in the cores of the pulsactors themselves. This power loss, due to eddy currents, is a function of the type of material used in the core, and the thickness of the laminations.

In an effort to keep these losses to a minimum, these laminations are as thin as is feasable. However, due to limitations imposed by the core material itself in the manufacture of these units, thicknesses of less than two mils are not often available.

The computation of this core loss is empirical in form, and depends upon the engineer having data available in curves of loss vs. frequency. A typical curve is shown in Figure 47.

In addition to core loss, a finite resistance is met in the wire used to wind the coils, and connect the components. The effect of this resistance is studied in this chapter. It has been determined experimentally that a $Q = 3$ can be obtained in all of the circuits using the pulsactors as switching devices.

The first stage of the magnetic modulator as shown in Figure 18 is analyzed from this circuit Q point of view, where $Q = \frac{\omega_o L_e}{R}$.

Letting $n_1 = 1$, for simplicity, and $L_1$ being an ideal transformer, the equivalent circuit of the first stage is as noted in Figure 31.

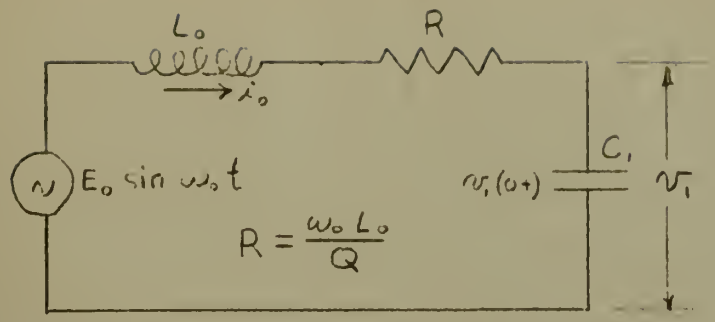


Figure 31. Schematic Diagram of First Stage.

The initial conditions are: $i_o = 0$, $v_1\ (0+) = 0$.

We can immediately write $\left[L_o s + \frac{\omega_o L_o}{Q} + \frac{1}{C_1 s}\right] I = E_o \frac{\omega_o}{s^2 + \omega_o^2}$

$$\therefore \quad I = \frac{E_o \omega_o}{s^2+\omega_o^2} \times \frac{s}{L_o} \times \frac{1}{s^2 + \frac{\omega_o}{Q} s + \frac{1}{L_o C_1}}$$

or, $$I = \frac{E_o \omega_o}{s^2+\omega_o^2} \times \frac{s}{L_o} \times \frac{1}{(s+\frac{\omega_o}{2Q})^2 + \left(\sqrt{\frac{1}{L_o C_1} - \frac{\omega_o^2}{4Q^2}}\right)^2}$$

Now, let $\alpha = \frac{\omega_o}{2Q}$ , $\beta^2 = \omega_o^2 - \alpha^2$ , $\omega_o^2 = \frac{1}{L_o C_1}$

then, $$V_1 = \frac{I}{C_1 s} = \frac{E_o \omega_o^3}{(s^2+\omega_o^2)\left[(s+\alpha)^2 + \beta^2\right]}$$

$$\therefore \quad v_1 = E_o \omega_o^3 \frac{1}{\left[(\alpha^2+\beta^2-\omega_o^2)^2 + 4\alpha^2\omega_o^2\right]^{1/2}} \left\{\frac{1}{\omega_o} \sin(\omega_o t - \psi_1) + \frac{1}{\beta} \epsilon^{-\alpha t} \sin(\beta t - \psi_2)\right\} \text{---} \quad (1.357)$$

Where, $$\psi_1 = \tan^{-1} \frac{2\alpha\omega_o}{\alpha^2+\beta^2-\omega_o^2}$$

and $$\psi_2 = \tan^{-1} \frac{-2\alpha\beta}{\alpha^2-\beta^2+\omega_o^2}$$

Now $\beta^2 = \omega_o^2 - \alpha^2 = \omega_o^2\left(1 - \frac{1}{4Q^2}\right)$ and if Q is greater than 2, $\beta^2 \cong \omega_o^2$.

In that case, $v_1 = \frac{E_0 \omega_0^2}{\alpha (\alpha^2 + 4\omega_0^2)^{1/2}} \left\{ \left[ \sin (\omega_0 t - \tan^{-1} 4Q) \right] + \epsilon^{-\alpha t} \left[ \sin (\omega_0 t - \tan^{-1}(-4Q)) \right] \right\}$ ----- I

When $Q = 3$, and $\omega_0 t = 2\pi$, $v_1 = E_0 Q (.996)(1 - \epsilon^{-\pi/Q})$

or $v_1 = 1.945 E_0$ .....II

As has been previously noted, in the lossless case, $v_1 = \pi E_0$. It is then readily seen that the inclusion of some resistance in the circuit results in a marked change in the value that $v_1$ finally arrives to, in single cycle charging.

Substituting the values for $\alpha$ and $\beta^2$, we find that the angles $\psi_1$ and $\psi_2$ reduce to the following,

$$\psi_1 = \frac{\pi}{2} \quad , \quad \psi_2 = \tan^{-1} -\sqrt{4Q^2 - 1}$$

This will then result in the general expression for the voltage across the condenser $C_1$ being,

$$v_1 = Q E_0 \left[ \sin (\omega_0 t - \tfrac{\pi}{2}) + \frac{2Q}{\sqrt{4Q^2-1}} \epsilon^{-\frac{\omega_0 t}{2Q}} \sin \left( \frac{\omega_0}{2Q} \sqrt{4Q^2-1}\, t - \tan^{-1} -\sqrt{4Q^2-1} \right) \right]$$

A plot of the normalized voltage across the condenser, $\frac{v_1}{E_0}$ vs. the circuit factor, Q, for the time $t = \frac{2\pi}{\omega_0}$, appears in Figure 32.

It has already been shown that $\beta$ max occurs when $v_1$ is passing through zero. (Page 24, Chapter III) As $\int v_1 \, dt = -NA2\beta_{max}$ it is now of interest to show how the time, $\omega_0 t$, varies as a function of Q at the point where $v_1 = 0$.

It will be more convenient to express $v_1$ as a function of Q in a different form than the previous derivation, so let us now reconsider,

$$I = \frac{E_0 \omega_0}{L_0} \frac{s}{\left[ s + \frac{\omega_0}{2Q} \right]^2 + \left[ \sqrt{\frac{1}{L_0 C_1} - \frac{\omega_0^2}{4Q^2}} \right]^2} \times \frac{1}{s^2 + \omega_0^2}$$

Now, the circuit is to be adjusted so that, $\omega_0^2 = \beta^2$

Then, $v_1 = E_0 \omega_0 (\alpha^2 + \beta^2) \left\{ \frac{1}{\left[ \alpha^4 + 4\alpha^2 \beta^2 \right]^{1/2}} \left[ \frac{1}{\beta} \sin (\beta t - \psi_1) + \frac{1}{\beta} \epsilon^{-\alpha t} \sin (\beta t - \psi_2) \right] \right\}$

where $\psi_2 = -\psi_1$.

Taking advantage of the relationship,

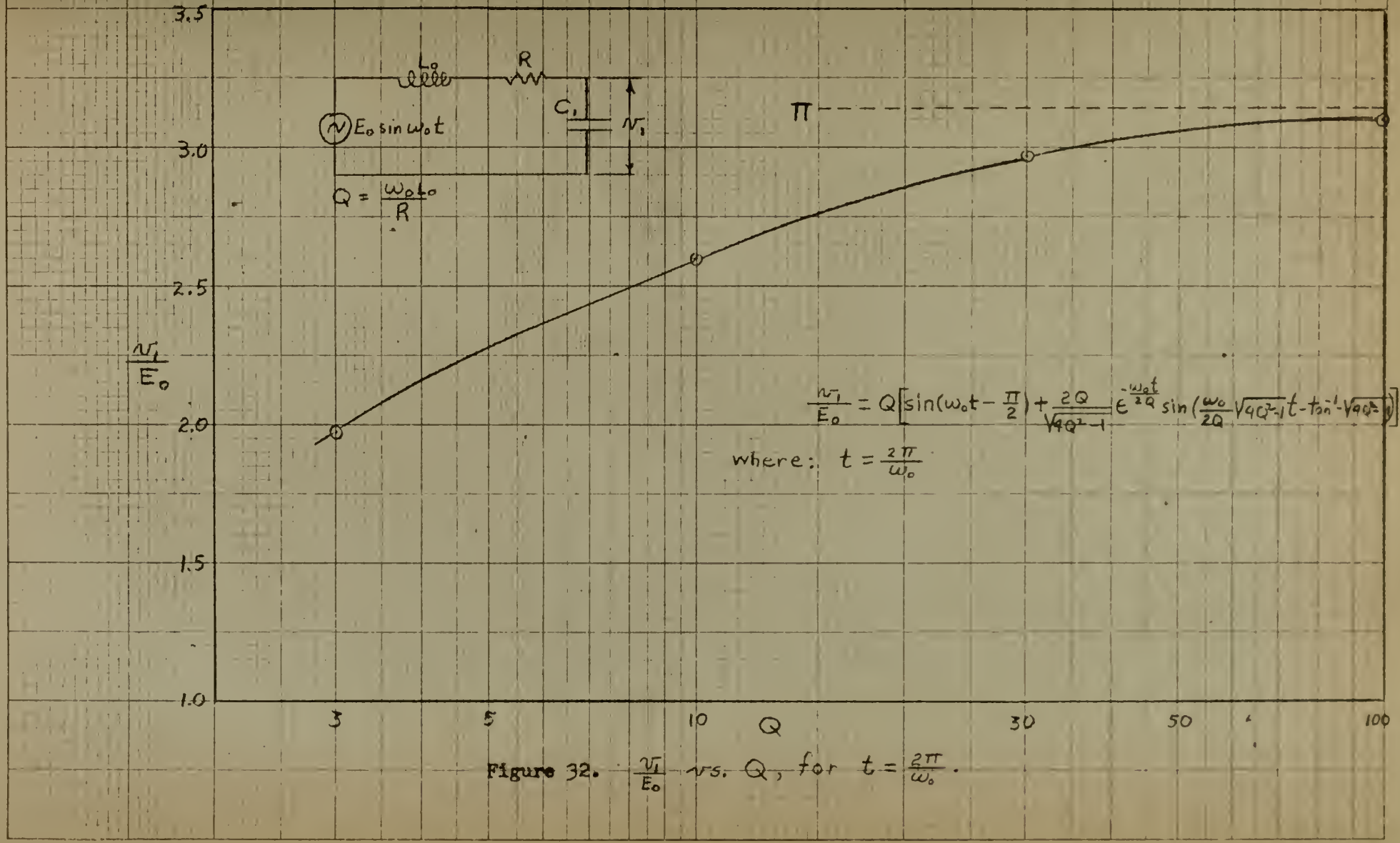


Figure 32. $\frac{V_1}{E_0}$ vs. Q, for $t = \frac{2\pi}{\omega_0}$.

$$\sin(A \pm B) = \sin A \cos B \pm \cos A \sin B$$

and substituting the values of $\cos\psi_1$ and $\sin\psi_1$ in the appropriate places,

$$v_1 = \frac{E_0\omega_0(\alpha^2+\beta^2)}{\alpha\beta}\left\{\frac{1}{(\alpha^2+4\beta^2)}\left[\alpha\sin\beta t(1+\epsilon^{-\alpha t}) - 2\beta\cos\beta t(1-\epsilon^{-\alpha t})\right]\right\} \qquad \ldots\text{III}$$

As $\alpha = \frac{\omega_0}{2Q}$, equation III can be reduced to

$$v_1 = E_0\left[\frac{1+4Q^2}{1+16Q^2}\right]\left[\sin\omega_0 t(1+\epsilon^{-\frac{\omega_0 t}{2Q}}) - 4Q\cos\omega_0 t(1-\epsilon^{-\frac{\omega_0 t}{2Q}})\right] \qquad \ldots\text{IV}$$

We are interested in the time, $\omega_0 t$, in equation IV, where $v_1$ passes through zero. By utilizing the relationships, $1+\epsilon^{-\frac{x}{2}} = \frac{2}{\epsilon^{x/4}}\cosh\frac{x}{4}$, and $1-\epsilon^{-x/2} = \frac{2}{\epsilon^{x/4}}\sinh\frac{x}{4}$ the expression that will finally give the criteria for solving for $\omega_0 t$ for the various values of Q, when $v_1 = 0$, is,

$$\tan\omega_0 t = 4Q\tanh\frac{\omega_0 t}{4Q} \qquad \ldots\ldots\ldots\ldots\text{V}$$

The results are plotted in Figure 33.

It is now of interest to find out what the $\int v_1\,dt$ is under the conditions as expressed in equation V. Integrating equation IV, we find that,

$$\int v_1\,dt = E_0\frac{1+4Q^2}{1+16Q^2}\left(-\frac{1}{\omega_0}\right)\left\{\cos\omega_0 t\left(1+\frac{12Q^2}{1+4Q^2}\epsilon^{-\frac{\omega_0 t}{2Q}}\right) + 2Q\sin\omega_0 t\left[2+\frac{\epsilon^{-\frac{\omega_0 t}{2Q}}}{1+4Q^2}(1-8Q^2)\right]\right\} \text{----VI}$$

Equation VI is plotted in Figure 34. This curve could now be used to compute the NA of the pulsactor.

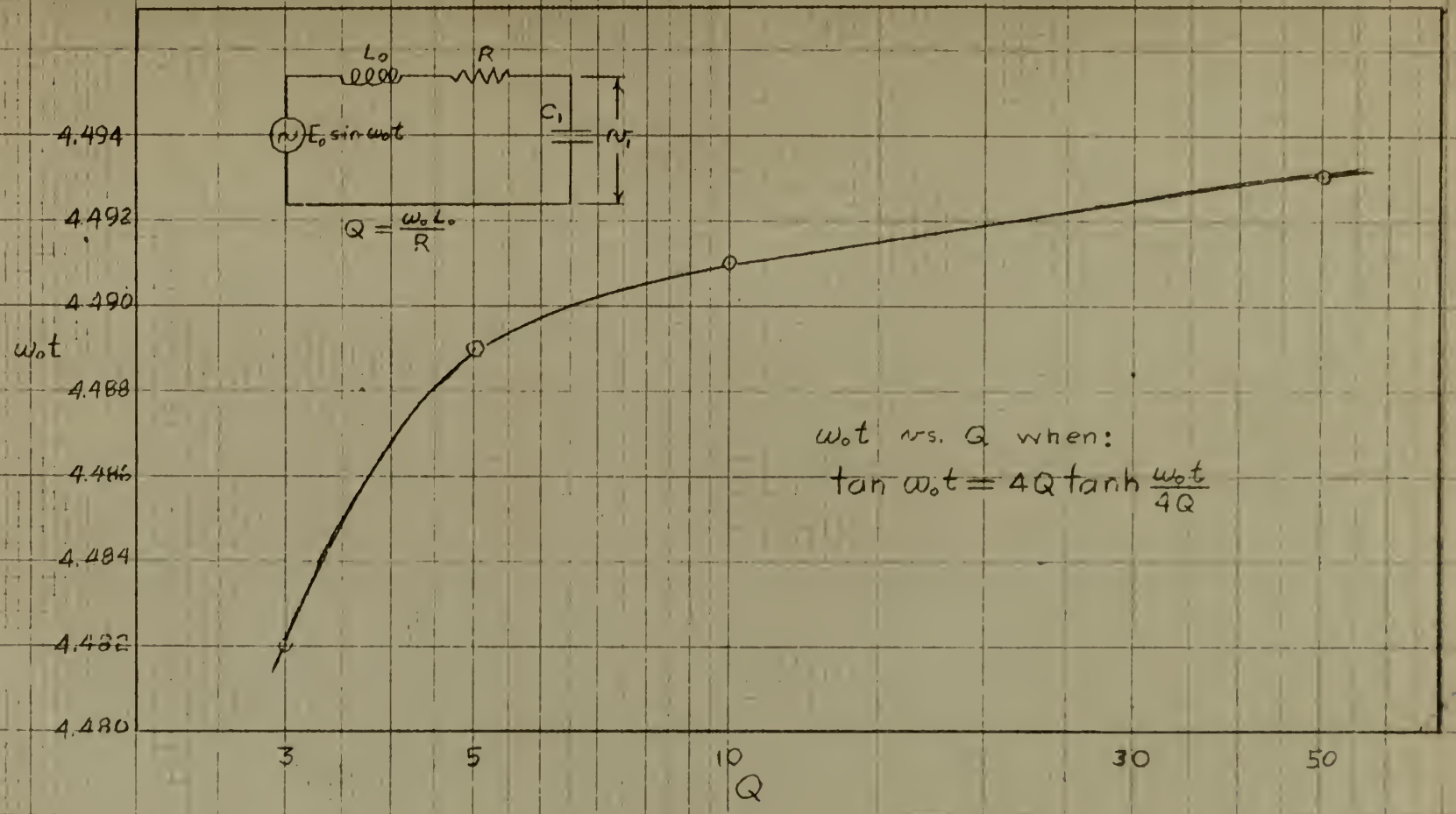


Figure 33. $\omega_o t$ vs. Q, for $\frac{v_1}{E_o} = 0$

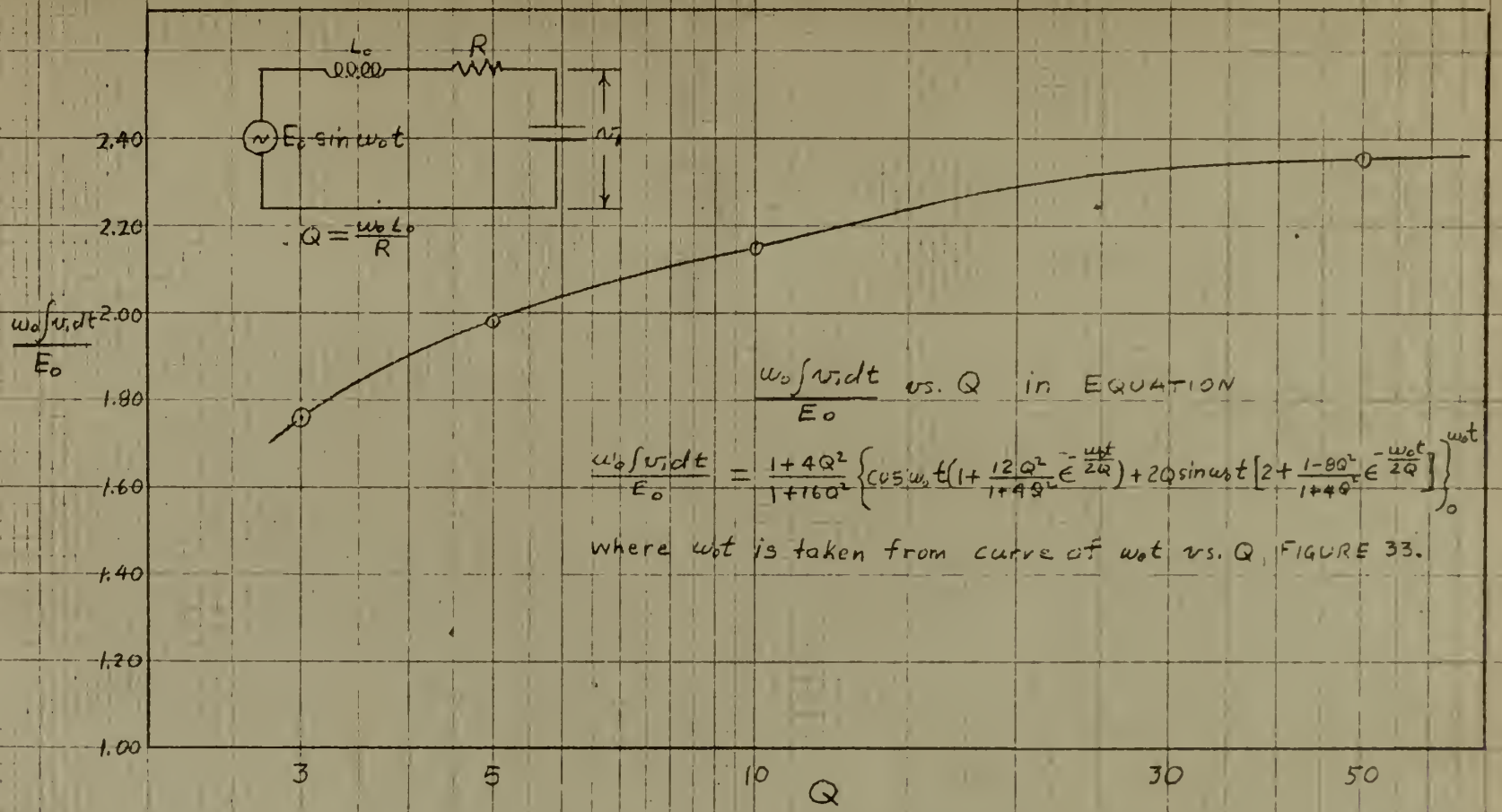


$\frac{\omega_o \int v_i dt}{E_o}$ vs. Q in EQUATION

$$\frac{\omega_o \int v_i dt}{E_o} = \frac{1+4Q^2}{1+16Q^2}\left\{\cos\omega_o t\left(1+\frac{12Q^2}{1+4Q^2}\epsilon^{-\frac{\omega t}{2Q}}\right)+2Q\sin\omega_o t\left[2+\frac{1-8Q^2}{1+4Q^2}\epsilon^{-\frac{\omega_o t}{2Q}}\right]\right\}_0^{\omega_o t}$$

where $\omega_o t$ is taken from curve of $\omega_o t$ vs. Q FIGURE 33.

**Figure 34.** $\frac{\omega_o \int v_i dt}{E_o}$ vs. Q.

# CHAPTER V

## DESIGN CONSIDERATIONS

Chapters III and IV have been concerned with the behavior of the circuit in general, and with determining the values required of the various components. As yet, nothing has been said as to how these values are to be obtained. This chapter will show how the wire size is determined, the factors to consider in the windings of the toroids, as well as the determination of the bias current. In addition, an approach is made to pulse transformer design, and an analysis of the power factor in the lossless case studied. This is finally terminated with a short discussion of the core material used in the toroids.

It is now of interest to look at the waveforms of the current that flows in the first stage. The RMS value of this current will then determine the minumum wire size required. The schematic diagram of the first stage is shown in Figure 35. The initial conditions are $i_o = 0$, $C_1 = C_2$, and the charge on $C_2 = 0$. Then, $i_1$ is readily found to be,

$$i_1 = (-\pi n_1 E_o)\,\pi f_1 C_1 \sin \omega_1 t \qquad \text{.....VII}$$

Looking at the time plot of equation VII, with the time scale based on $\omega_o t$, note that the current flows in pulses, each pulse of half the sin wave frequency, $f_1$ and of duration, $\frac{1}{2 f_1}$. See Figure 36.

Using the basic definition of RMS current, $i_{rms} = \sqrt{\frac{1}{T}\int_o^T i^2 dt}$

$$i_{1\ rms} = (-\pi n E_o)\frac{\pi}{2} C_1 \sqrt{PRF \cdot f_1} \qquad \text{.....VIII}$$

Now, consider the current flowing in the primary side of the first stage, assuming an ideal transformer.

This is, $i_o = \frac{E_o}{2 L_o}\, t \sin \omega_o t$ .....IX

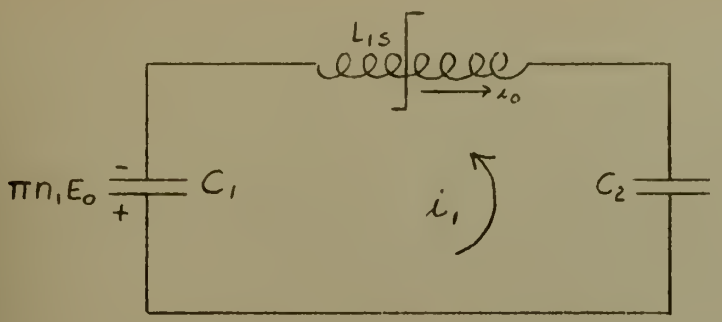


Figure 35. First Stage Schematic.

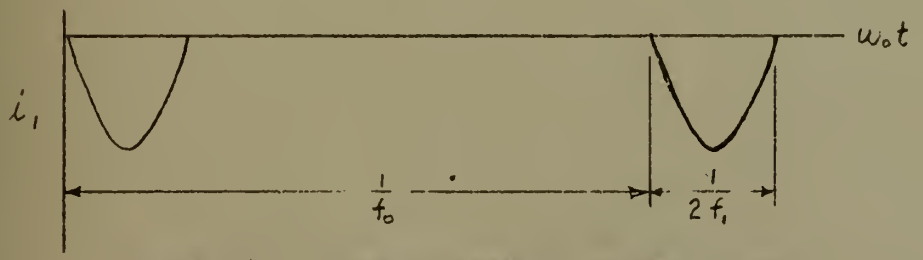


Figure 36. Current Waveform, First Stage.

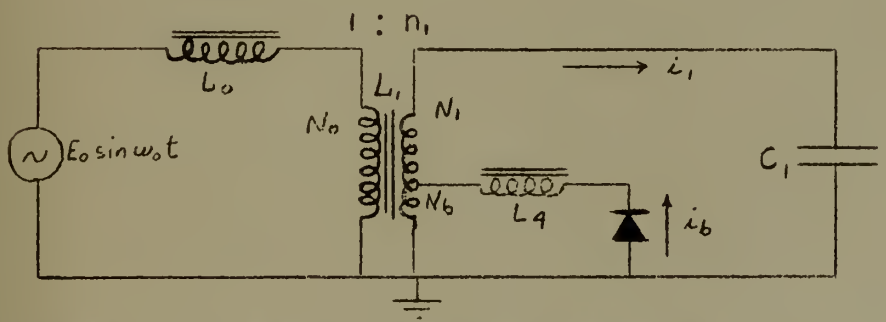


Figure 37. Schematic Diagram of Polarizing Circuit.

Once again, using the basic definition of RMS current, we find that

$$i_{o\ rms} = 7.90\ E_o f_o C_1 n_1^2 \quad \text{.....X}$$

Similarly, the current in the third stage can now be found. This is

$$i_{3\ rms} = 0.886\ v_3\ C_3 \sqrt{\frac{PRF}{\tau}} \quad \text{.....XI}$$

The current in the second stage, $i_{2\ rms}$, is of the same form as the expression for $i_{1\ rms}$, and therefore is equal to, $i_{2\ rms}$

$$i_{2\ rms} = (-\pi n E_o) \frac{\pi}{2} C_2 \sqrt{PRF \times f_2} \quad \text{.....XII}$$

The design criteria for the size wire to use, as practiced by North American Aviation, Inc., is to use 250 circular mils cross sectional area of copper wire for each ampere of RMS current. Lee, [3] in his text, has a chart in which circular mils per ampere are plotted against RMS volt-amperes. However, this is for continuous operation, not for pulsed networks, and is based upon a temperature rise that is quite a bit more conservative than is considered necessary for pulse operation.

Voltage breakdown, wire to wire, and layer to layer in the multilayer coils, must also be taken into consideration. A special type of insulated copper wire, made by General Electric, and known commercially as "Formex", or its equivalent, is recommended. This type of insulation gives a wire to wire voltage breakdown of better than 500 volts. As long as the voltage differential does not exceed this 500 volts, wire to wire, no additional insulation is considered necessary. If multiple layer windings are used, with the conventional separation of layers by using kraft paper, a breakdown level of 50 volts per mil thickness of the paper is considered sound design practice. The above figures on breakdown levels are all for the toroidal core being immersed in silicon oil, properly evacuated and sealed.

"Formex" wire has an insulating material consisting of a thin film of synthetic resin of polyvinyl-acetal. This insulating material does not

develop cracks from small radius bends, or disolve in the silicon oil.

As explained on page 10, it is necessary to have an average current, $I_B$, flowing in the pulsactor $L_1$, (See Figure 18) to obtain single cycle firing. The first step is then to determine what average current is required to obtain this necessary bias.

The schematic diagram of the equivalent circuit is shown in Figure 37. In this figure, $N_o$ is the number of turns on the primary side of $L_1$, $N_1$ is the number of turns on the secondary, and $N_b$ is the number of turns from the tapped part of the secondary to ground. From Figure 37, it can be determined that,

$$i_b = \left(\frac{N_b}{N_o}\right)\left(\frac{E_o}{L_4}\right)\omega_o^3\left[\frac{1}{\omega_o^4}(1-\cos\omega_o t)-\frac{1}{2\omega_o^3}t\sin\omega_o t\right] \quad \text{.....XII}$$

From the basic definition of an average current, $i_{avge}=\frac{1}{T}\int_o^T i_b\,dt$, it can then be determined, that,

$$i_{avge}=\left(\frac{N_b}{N_o}\right)\frac{3}{2}\frac{E_o}{\omega_o L_4} \quad \text{for one cycle charging.....XIII}$$

Also, $i_{1\ avge}=\frac{Q}{t_o}=C_1\left(\frac{N_1}{N_o}\right)\pi E_o f_o$ .....XIV

Now, as $i_{b\ avge} \times N_b = i_{1\ avge} \times N_1$,

$$L_4=\frac{3}{C_1\omega_o^2}\left(\frac{N_b}{N_1}\right)^2 \quad \text{.....XV}$$

Let $L_e$ be the effective inductance across the secondary.

Then $L_e=\frac{L_4\left(\frac{N_1}{N_b}\right)^2 L_o\left(\frac{N_1}{N_o}\right)^2}{L_4\left(\frac{N_1}{N_b}\right)^2+L_o\left(\frac{N_1}{N_o}\right)^2}$ .....XVI

Also, $L_e=\frac{1}{\omega^2 C_1}=\frac{1}{\alpha^2\omega_o^2 C_1}$ .....XVII

where $\omega_o$ is the input frequency, $\omega$ is the resonant frequency, and $\alpha=\frac{\omega}{\omega_o}$.

Equating XVI and XVII equation XVIII is then obtained.

$$L_o=\frac{3}{(3\alpha^2-1)C_1\omega_o^2\left(\frac{N_1}{N_o}\right)^2} \quad \text{.....XVIII}$$

It has been found that for maximum output, $\alpha = 1.25$.

Equation VI, page 25, used in computing the inductance of a saturated pulsactor, is quite adequate as long as the toroid is wound for a full 360° of arc, with a single layer of wire. When working with relatively high voltages, as is the case in the magnetic modulator, it is not feasable for the high and low ends of one winding to be immediately adjacent to each other, or voltage breakdown will occur. As this separation is required, it is not possible to wind these toroids a full 360°. To predict what the inductance will be under these conditions, what this writer calls a "toroidal winding factor", k, will be used. This is defined as follows: $k = \frac{L_m}{L_s}$, where $L_s$ is the normal or "standard" value of inductance, and is computed from equation VI, page 25. $L_m$ is the inductance of toroid when the winding occupies some degree of arc other than 360°. The factor k is plotted vs. the degrees of arc of the toroidal winding in Figure 38. By knowing the dimensions of the pulsactor, $L_s$ can then be computed. By knowing the degrees of arc the winding will occupy, k can be selected from Figure 38. Then $L_m = k\ L_s$.

The design of the final stage depends upon how much leakage inductance is present in the pulse transformer. This problem of proper design of the pulse transformer is the most nebulous factor in the engineering of a magnetic modulator. In the design of $L_1$, the amount of leakage inductance was ignored. This could safely be done, as the relative values of $L_1$ and the leakage inductance present, are so far apart in magnitude. However, in the transformer $T_1$, such is not the case. The total inductance, required by the final stage is of the order of micro-henries, and

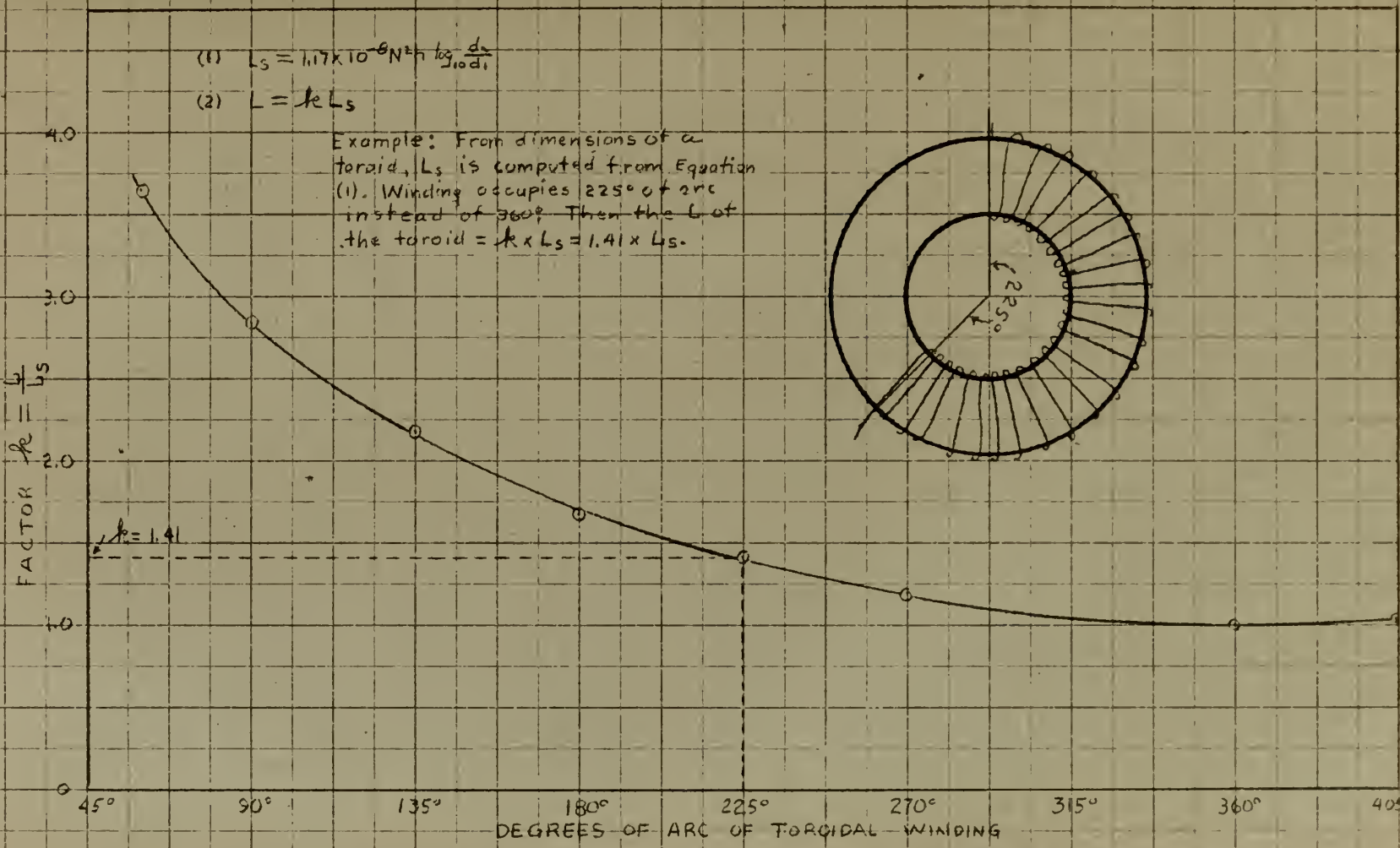


Figure 38. Plot of Toroidal Winding Factor vs. Degrees of Arc of Winding.

so is the leakage inductance, so that the orders of magnitude are about the same, and this leakage cannot be disregarded.

No attempt is made here to review all the considerations of estimating this leakage inductance. The word "estimate" is used with malice aforethought, as any computations of a design will give you only some approximation of the leakage L present. It will vary from one transformer to another, even when they are all of the same design.

One approach to the first step of the design is the procedure that follows. Consider Figure 39. This is a plot of L vs. $\mu$ for two different equations. In this figure, $L_a$ is the inductance of saturated pulsactor, as given by $L_a = 1.17 \times 10^{-8} N^2 h \log_{10} \frac{d_2}{d_1}$ . (See equation VI, page 25). $L_u$ is the inductance of a toroid when wound around a core with a characteristic $\mu$, and is given by $L_u = \frac{.4\pi N^2 \mu A}{\ell} 10^{-8}$. $L_e$ is the effective inductance of the toroid at any $\mu$. $L_D$ is the leakage inductance. $\ell$ is the mean magnetic path length of the core.

Now, as the pulse transformer is not normally wound a full 360° of arc, the toroidal winding factor, k must be introduced. Considering both the primary and secondary sides of the transformer,

$$L_D = L_{a\ \text{primary}} - L_{\substack{u=1 \\ \text{primary}}} + \frac{L_{a\ \text{secondary}} - L_{u=1,\ \text{sec.}}}{n_2^2} .$$

Then, by the proper substitution in the above equation,

$$L_D = N_1^2 \times 10^{-8} \left[ 1.17 \left( k_p h_p \log \left(\frac{d_2}{d_1}\right)_p + k_s h_s \log \left(\frac{d_2}{d_1}\right)_s \right) - \frac{0.8\pi A}{\ell} \right] \qquad \text{.....XIX}$$

As a check on the validity of the assumption that the leakage $L = L_D$, several pulse transformers that were previously constructed were used, to compute from equation XIX the leakage inductance, and then com-

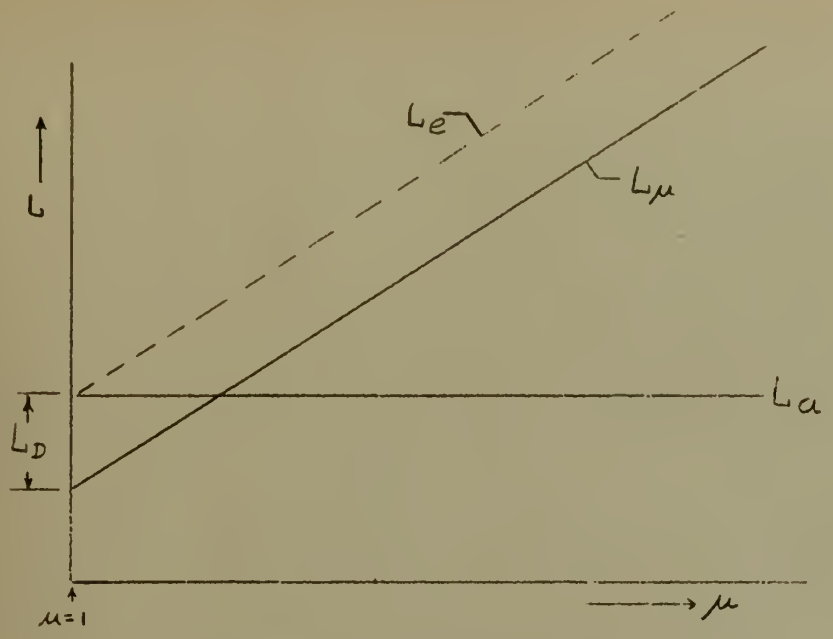


Figure 39. Plot of L vs.$\mu$.

| TRANSFORMER NO. | $L_D$ (COMPUTED) | $L_D$ (MEASURED) |
|---|---|---|
| #1 | 2.8 $\mu$h | 1.6 $\mu$h |
| #2 | 11.3 $\mu$h | 5 to 14 $\mu$h For Several "identical" pulse transformers. |
| #3 | 15.6 $\mu$h | 16.1 $\mu$h |

Table 1. Comparison of $L_D$ Computed and $L_D$ Measured.

pare the result with the measured leakage as measured on a bridge. The results are compared in Table 1.

At first glance, the above method would not indicate very good results. Familiarity with pulse transformer design would show that being in error by a factor of two to one, as far as leakage inductance is concerned is considered as quite adequate for design purposes. In any case, the procedure as noted above will provide a good starting point for laboratory "cut and try" redesign.

By making certain assumptions it becomes feasable to compute the theoretical power factor in the lossless case. The following equation is taken as the basic definition of power factor.

$$P.F. = \frac{\frac{1}{T}\int_0^T e_o i_o \, dt}{i_{o\,rms} \times E_{o\,rms}} \qquad \text{.....XX}$$

We are then able to substitute the known quantities into this equation, and compute the power factor, P.F. In this computation, the voltages and currents are those that exist in the charging circuit.

These known quantities are:

$e_o = E_o \sin \omega_o t$, the assumed input generator.

$i_o = \frac{E_o}{2L_o} t \sin \omega_o t$ , from equation IX, page 40.

$i_{o\,rms} = 7.90\, E_o f_o C_1 n_1^2$, from equation X, page 41.

$E_{o\,rms} = \frac{E_o}{\sqrt{2}}$.

$T = \frac{2\pi}{\omega_o}$.

$\frac{1}{T} = f_o$.

Direct integration of equation XX will then give,

$$P.F. = \frac{\pi^2}{2 L_o \omega_o^2} \times \frac{\sqrt{2}}{7.90\, C_1 n_1^2}$$

But, $\omega_o^2 = \frac{1}{L_o C_1 n_1^2}$

Therefore, P.F. = 0.8834 .....XXI

This is then the theoretical power factor in a lossless case, assuming the $i_o$ of the charging circuit is the complete current of the complete circuit. Some attempt to solve for the power factor in the circuit, with losses, has also been made, but the expressions so far resulting, have been too complicated to properly evaluate. In general, however, as the losses increase, the power factor tends to go up in value. It has been found in practice, that power factors greater than .90 are attained.

It is felt that a few comments on the characteristics of the core material used in the toroidal pulsactors should be made at this point.

The material that most closely approaches the requirements, as noted by Melville, [5] for a saturable core, (i.e. 1. Rectangular hysteresis loop, and 2. Thin rolled strips.) is found in a nickel-iron alloy. This material is sold commercially under the names of "Deltamax", "Orthonol", "Orthonik", "Permeron", "Hypernik V", depending on the manufacturer.

The alloy is in toroidal form only. There has been some attempt to make "C" cores, but this project has not met with much success. In the toroidal form, a continuous tape is wound cylindrically to form the familiar toroid shape. This tape will vary in thickness from 1 mil to 5 mils. The alloy is grain oriented, requiring precise annealing procedures. Unfortunately, it is strain sensitive, and must be so mounted that this factor will not enter into the problem. The cores are also expensive, small cores running about $0.90 per gram, with the larger cores

varying from $0.04 to $0.07 per gram. The core is usually encased in a plastic container and packed with silicon grease, so as to minimize the strain effects, as well as protecting it from handling and subsequent winding.

Very little A.C. data has been published. However, DC, 60 cycle, and 400 cycle AC characteristics, as published by manufacturers of the cores are noted in Figure 40.

Nickel is a critical material, and might, under conditions of national emergency, constitute a limiting feature of these toroids in the use of a magnetic modulator.

The effect of temperature on the hysteresis loop is not well known. The only statement that can be made at the present time, is that these cores do operate satisfactorily. The temperature of some of the cores, in the vicinity of a "hot spot", runs in the vicinity of 200° centigrade between laminations.

Known ambient temperature effects are noted in Figure 41.

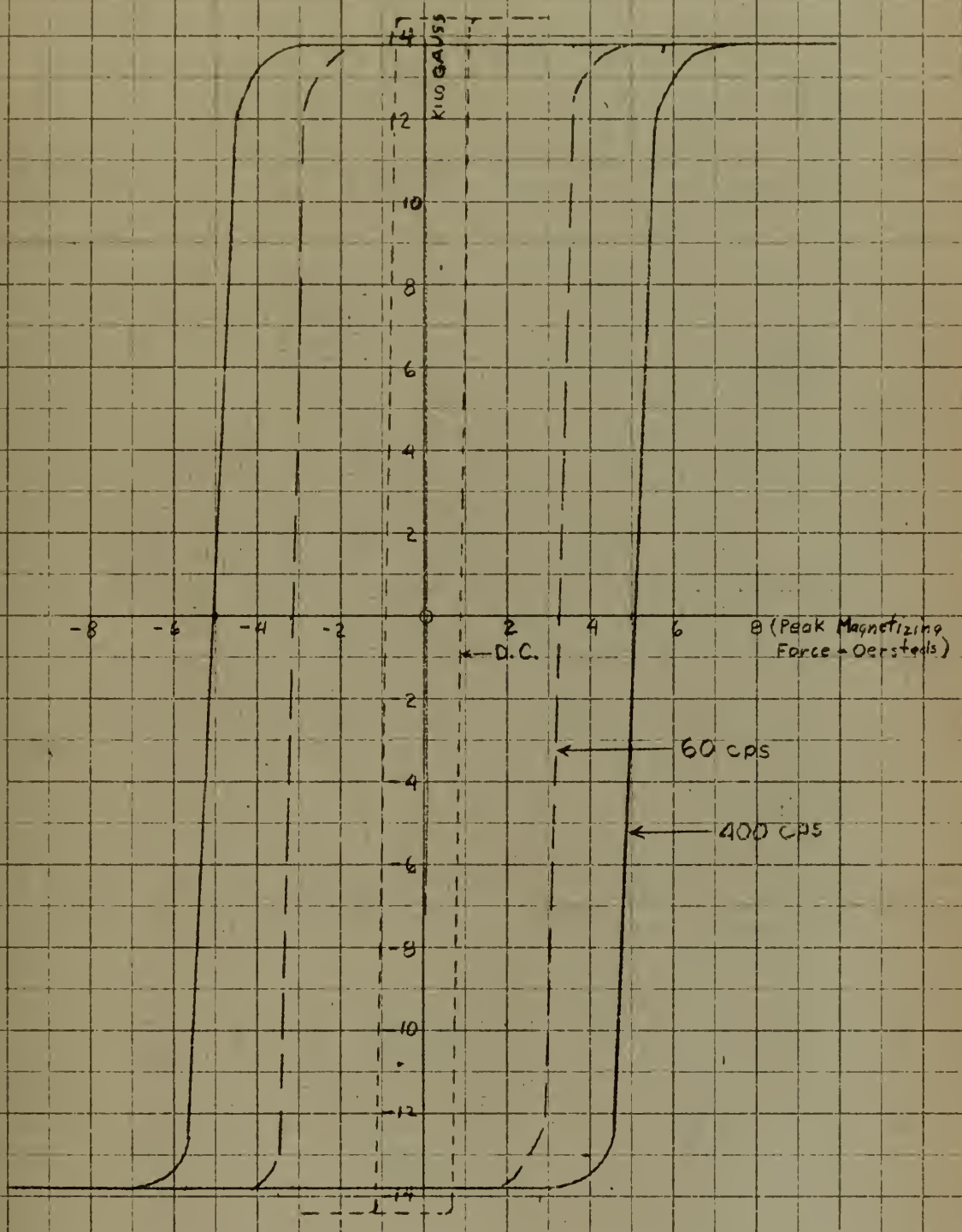


Figure 40. B/H Loop Characteristic of Pulsactor Core Material.

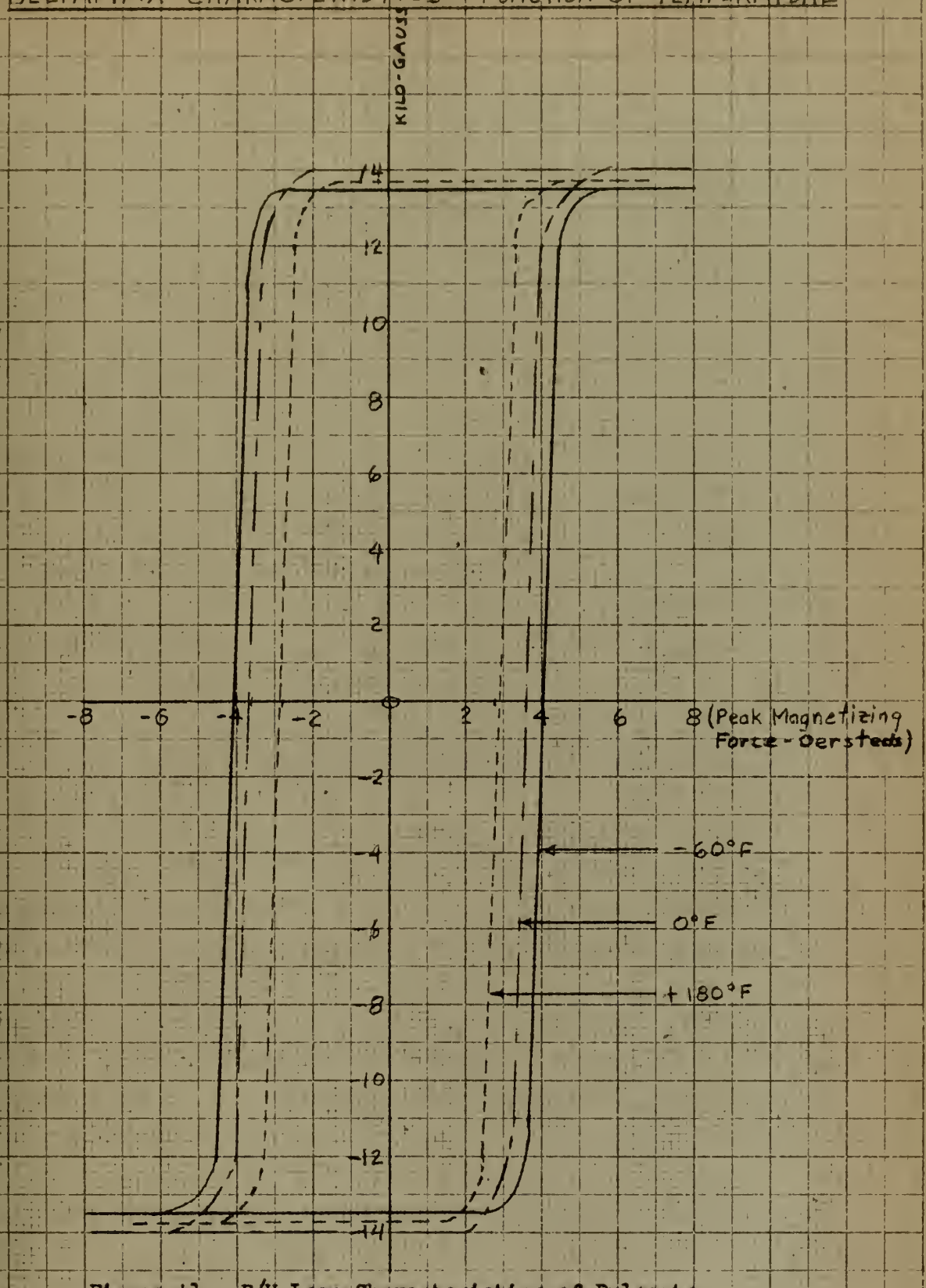


Figure 41. B/H Loop Characteristics of Pulsactor Core Materials, as a Function of Temperature.

# CHAPTER VI

## DESIGN OF A MAGNETIC MODULATOR

The specifications of a typical radar of high power were taken from the APS-20(E). These specifications were modified to a certain extent in relation to the PRF and selectivity of pulse width, to ease the requirements of the modulator, and still show the way the design may be attacked.

In particular, the PRF of the present APS-20(E) is 300. This relatively low PRF is required due to the presence of the data link. It is not intended that this paper should go into the requirements of a data link for radar presentation, but it is felt that this particular system is very wasteful of the time domain to fulfill the requirements desired. (i.e. Data link must transmit a synchronization pulse, azimuth information and the video of the radar.) For particulars on this phase, the reader is referred to the Handbook of Maintenance Instructions for the APS-20 (A), (B), or (E).

The APS-20(E) also has provisions for the operator to select a second PRF and pulse width of 900 and 0.6 micro-sec. respectively. To fulfill this requirement on a magnetic modulator design would be to repeat the design of the first modulator for a different PRF and pulse width. It is not felt that any value would lie in doing this. The writer did desire to point out that the design as given here does not fit the complete requirements of the APS-20(E).

The specifications selected to design a modulator unit are:

RF Power Out = $2 \times 10^{6}$ watts peak = $P_t$

$\tau = 2 \times 10^{-6}$ seconds

$f_o = 400$ cps

PRF $= 400$ pps

Eo $= 115\sqrt{2} = 163$ volts peak

The magnetron used in this case is the QK-428, in which,

Imag $= 85$ amps., and

Emag $= -61.5 \times 10^3$ volts.

The maximum range to be presented by the radar unit is 200 nautical miles.

At PRF $= 400$, the time of one cycle $= 2500$ micro-secs

200 Mile range $= 200 \times 12.3 =$ 2460 " "

Time allowed for data link $=$ 40 " "

It is realized that the above puts stringent requirements on the data link system.

1. Efficiencies:

Based upon past experience by the engineers at North American Aviation, the following efficiencies of each stage are assumed.

$\eta_1 =$ (input and first stage) $= 0.8$

$\eta_2 =$ (second stage) $= 0.9$

$\eta_3 =$ (third stage) $= 0.9$

$\eta_p =$ (pulse transformer) $= 0.9$

$\eta_t =$ (transmitter tube) $= \dfrac{2 \times 10^6}{85 \times 61.5 \times 10^3} = 0.382$

Overall efficiency, $\eta = \eta_1 \cdot \eta_2 \cdot \eta_3 \cdot \eta_p \cdot \eta_t$

$\eta = 0.223$ or 22.3%

2. Determination of charging stage current.

$[P_t \tau]400 = \eta \dfrac{Eo\ Io \times P.F.}{\sqrt{2}}$ where Io = charging current, RMS

P.F. = Power Factor = 0.9(Assumed)

then $Io = \dfrac{P_t \tau\ 400\sqrt{2}}{\eta\ Eo\ P.F.} = \dfrac{(2 \times 10^6)(2 \times 10^{-6})400\sqrt{2}}{163\ (.223)(0.9)}$

Or Io = 69.1 amps.

3. Determination of capacitor size, and maximum voltage peak.

Now $\frac{\eta C v_1^2}{2} = P_t \tau$ where $v_1$ = voltage across $C_1$.

At this point a decision as to selecting either C or $v_1$ must be made. It is felt that $25 \times 10^3$ volts should not be exceeded, as above that, the breakdown and corona problems become difficult, and indeed, it is bad enough at the 25 kilo-volt level. Then C is usually obtained in some integer value such as .1, .01, or .05 micro-farads, and not 0.0197 micro-farads. One or two trial computations will show in what vicinity C should then be selected so as not to have $v_1$ be excessively high. In this particular case,

C = 0.06 Micro-farads,

then $v_1 = 24.4 \times 10^3$ volts,

as $v_2 = \sqrt{\eta_1}\, v_1$, then $v_2 = 21.8 \times 10^3$ volts

similarly, $v_3 = 20.7 \times 10^3$ "

and $v_p = \frac{2}{e}\sqrt{\eta_1 \eta_2 \eta_3}\, v_1 = 14.45 \times 10^3$ volts (see eq XIV, page 30.)

4. Frequency step up per stage.

Freq. step up per stage $= \frac{1}{\sqrt[3]{2 \tau f_o}} = 8.55.$

Experience has shown that it is wise to have as little frequency multiplication as possible in the last stage. This helps to keep the losses down, as the losses increase as the frequency goes up. It is then necessary to have more multiplication of frequency in the first two stages. Arbitrarily, the first stage is then increased by the factor $\sqrt[3]{2}$.

then $f_1 = \frac{fo\sqrt[3]{2}}{\sqrt[3]{fo\ 2\tau}} = 4.310 \times 10^3$ cps.

5. Determination of $N_1 A_1$ of the first stage.

By referring to the middle line of $\beta$ max. vs. frequency curve for

"deltamax", as given in Figure 47, it is found that at a frequency of 4.31 kc, $\beta$ max. = $1.33 \times 10^4$ gauss per $cm^2$.

For a Q = 3, $E_{c1} = 2Eo\ n_1$ (See Equation, page 35.)

Also that $N_1A_1 = \left(\frac{Eo}{\beta max.\ fo}\right) \times \left(\frac{3.4}{4\pi}\right) \times 10^8$ (See Equation V, page 25.)

therefore $N_1A_1 = \left(\frac{E_{c1}}{2\beta_{MAX}\ f_o}\right)\left(\frac{3.4}{4\pi}\right)10^8$

$= 6.21 \times 10^4$

Now $L_1$ (air core) $= 1.17 \times 10^{-8} N_1^2\ h_1 \log\left(\frac{d_2}{d_1}\right)$

and, from the previous equation, $N_1 = 6.21 \times 10^4 \frac{1}{A_1}$

then, $L_1$ (air core) $= 45.1\left[\frac{h_1}{A_1^2} \log_{10}\left(\frac{d_1}{d_1}\right)\right]$

Also, from the requirements of the circuit, $L_1$ (air core) $= \frac{1}{2\pi^2 f_1^2 C_1} = 45.4$ mh

Then $K_1 = \left[\frac{h_1}{A_1^2}\right] \log_{10}\left(\frac{d_2}{d_1}\right) = 0.001005.$

The characteristic K of any given core can be catalogued in this term. If this is done, you will find that there is not a standard core with this K factor = .001005. You must then compute the dimensions of the required core.

Initially, certain assumptions are made.

1. That the cross section of the core is square.

2. That $d_2 = 5h$, and that $d_1 = 3h$. (See Figure 42.)

then $\frac{h}{A^2} = \frac{h}{h^4(6.452)^2}$, if h is expressed in inches, and A in inches squared.

Now, $1.005 \times 10^{-3} \doteq \frac{1}{h^3\ (41.7)}\ (0.222)$

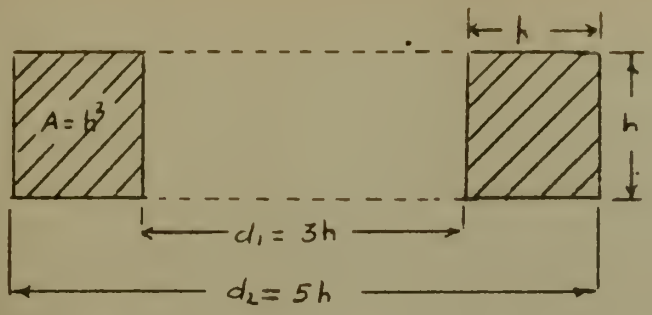


Figure 42. Relative Dimensions of Pulsactor Core.

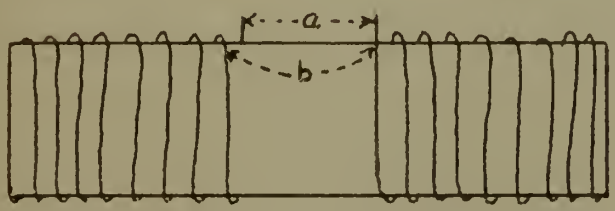


Figure 43. Voltage Breakdown Paths in Pulsactor Core

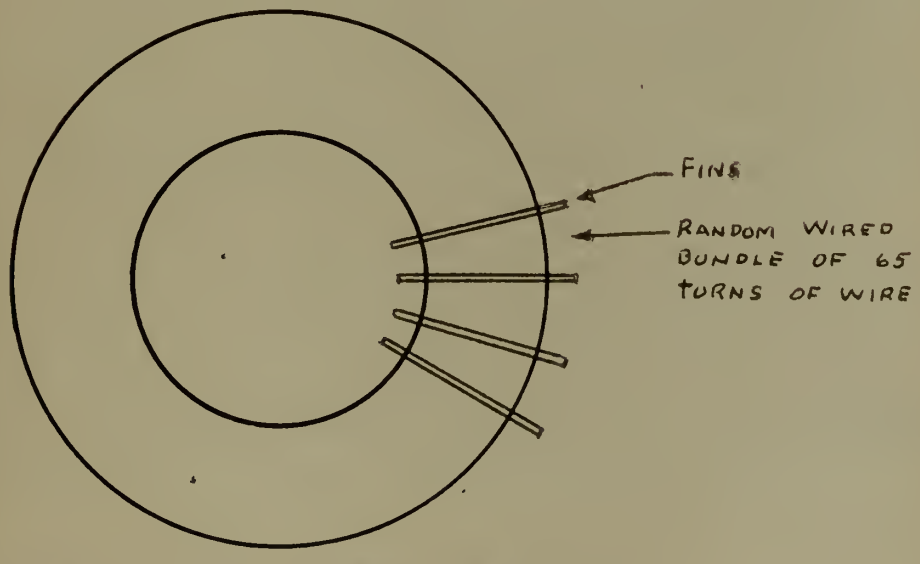


Figure 44. Typical First Stage Pulsactor.

or $h = 1.74"$

then, $A = 19.5$ cm.$^2$, $d_1 = 5.22"$, $d_2 = 8.71"$. This then, is the bare dimensions of the core. This must be enclosed in a protective case.

Now $N_1A_1 = 6.21 \times 10^4$, and $A = 19.5$ cm.$^2$,

therefore $N_1 = 3180$ turns.

In the computation of the dimensions of the core above, it is obvious that h, A, $d_1$, and $d_2$ are computed on the basis of a bare core alone. As mentioned above, the core must be encased in a protective cover. This, in turn, must be wrapped with insulating tape to prevent the turns from shorting out to the core itself, due to voltage breakdown. All this, plus the fact that with the large number of turns required by the secondary, a multiple layer winding will be required, invalidates the initial determination of h, $d_1$ and $d_2$ by a considerable factor. It is not intended to show the trial and error computation this author went through to finally determine the correct size core. Suffice it to say, that the approach as given above was accomplished initially, and then constant revisions were necessary before the core, as finally designed, was computed.

Let us first look at the insulation that must be wrapped around the core. There are two main paths for a voltage breakdown to occur in a toroidal core.

(a) From one end of the winding to the other end, through the oil insulation surrounding the core.

(b) From one end of the winding, down through the insulating material to the core, thence along the core, (or through it) to the other end of the winding. See Figure 43.

If a glass type tape is used for insulating the case from the wire, it will withstand 300 volts per mil of insulating material. The insulating material comes in tape 3 mils in thickness. It will now be necessary to compute how many layers will be necessary to withstand the voltage used.

Using a safety factor of two, and considering the case as contributing nothing towards insulation of the core, the number of layers of 3 mil tape = $\frac{24.4 \times 10^3}{900} = 27$ layers.

The thickness of the insulating tape = 81 mils.

The case thickness of a core of this size = 162 mils.

Therefore, the dimensions of the core as initially computed, must now be modified by these factors.

The diameter of the wire that will be used to carry the current $= \sqrt{250} \times \sqrt{I_o} = 132$ mils. This results in a wire size of AWG #7, which has a diameter of 0.1501 inches, with insulation.

6. RMS current in the secondary.

The RMS current in the secondary $= \frac{\pi}{2} \cdot C\ v_1\ \sqrt{PRF \times f_1}$ (See equation VIII, page 40.) This current is due to the action of the switching and frequency multiplication of the first stage only. In addition to this, the charging current as given previously must also be taken into consideration, or $I_o$ (Secondary) $= \frac{N_o}{N_1}\ I_o$.

The worst condition of current would be when both currents are present at the same time. As, by definition, the RMS value is that which will give the same heating effect as the pulsed current, the sum of these two is taken for design purposes of determining wire size.

Therefore, $I_1 = \frac{N_o}{N_1}\ I_o + \frac{\pi}{2}\ C\ v_1\ \sqrt{PRF \times f_1}$

$$I_1 = 3.94 \text{ amps.}$$

Then, the diameter of the wire is $=\sqrt{250} \times \sqrt{3.94} = 31.4$ mils. Referring to the wire chart, you will find this will then require AWG #20 wire, with the diameter with insulation = 34.5 mils.

Some discussion of the winding of multiple layer cores is now in order. In winding these cores on a toroidal core winding machine, it is necessary to assume that unless you are using single layer winding, the windings will be random wound. In other words, there will be a certain number of cross overs present, and you are unable to control the voltage differential wire to wire. As has been previously stated, the maximum allowable voltage wire to wire is 500 volts. The problem is then to prevent, under random wiring conditions, this value being exceeded.

If you separate the wiring into separate units, where each unit has only 500 volts gradient in it, and then insulate these units from each other, the objective will be attained. Let us call each one of these units a "bundle". Then, in the case under consideration, there will be $\frac{500 \times 3180}{24.4 \times 103} = 65.3$ turns per bundle. Or you can see that we will need 49 of these bundles. The insulating material between these bundles must withstand 1000 volts. Using MM "Glastic" or similar material, 1/32 in. thick, which will withstand 9000 volts, the bundles are adequately insulated. For mechanical strength reasons, it is necessary to use such thick material. This insulating material, called "fins" is held in place by a notched locking base on the inside and outside periphery of the core. This locking base can be made of polyester impregnated glass fabric, or material with similar characteristics. A sketch of a typical core with these fins, is included, to illustrate the above explanation; see Figure 44.

The random wired bundles build up the effective height of the toroid, as the several layers are wound on, and the L of the equivalent air core toroid changes from that computed on the bare core. A general case is now considered and how the h, $d_1$ and $d_2$ change as a winding is put on the core is computed. Referring to Figure 45, assume $x_1$, $x_2$, $y_1$, $y_2$ are straight lines.

Then, $A_1 = \frac{H_1}{2} ( x_1 + y_1)$

$A_2 = \frac{H_2}{2} ( x_2 + y_2)$

Also, for random wiring in $A_1$, with a smaller area than $A_2$, a stacking factor = 2 is used. As the surface $x_2$ is wider, and more even winding is then possible, assume ideal stacking. For convenience, also assume that square wire of diameter = d is being used.

Then, $A_1 = 2\, d^2\, N$

$A_2 = d^2\, N$ where N is the number of turns per bundle.

From similar triangles, $\frac{ID}{ID - H_1} = \frac{x_1}{y_1}$, or $y_1 = \frac{x_1 (ID - H_1)}{ID}$

$$A_1 = \tfrac{1}{2} \tfrac{H_1 x_1}{ID} \left[2(ID) - H_1\right] \quad , \quad \therefore \; H_1^2 \left[\frac{x_1}{2\,ID}\right] - H_1 [x_1] + A_1 = 0$$

$$\therefore \quad H_1 = ID \pm \sqrt{ID^2 - \frac{2 A_1 ID}{x_1}}$$

As $H_1 < ID$, $\quad H_1 = ID \left(1 - \sqrt{1 - \frac{2A_1}{ID\, x_1}}\right)$

Similarly, $\quad H_2 = OD \left(\sqrt{1 + \frac{2A_2}{OD\, x_2}} - 1\right)$

It is now possible to compute the H's and the x's of each bundle. The loss of circumference due to the presence of the fins must be taken

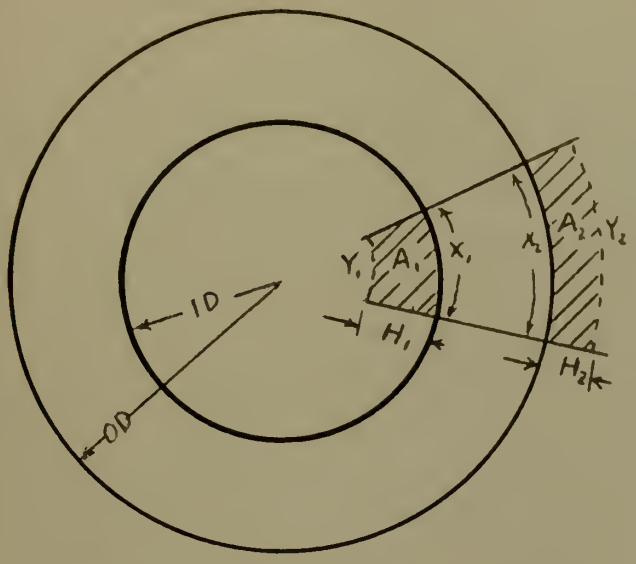


Figure 45. First Stage Pulsactor.

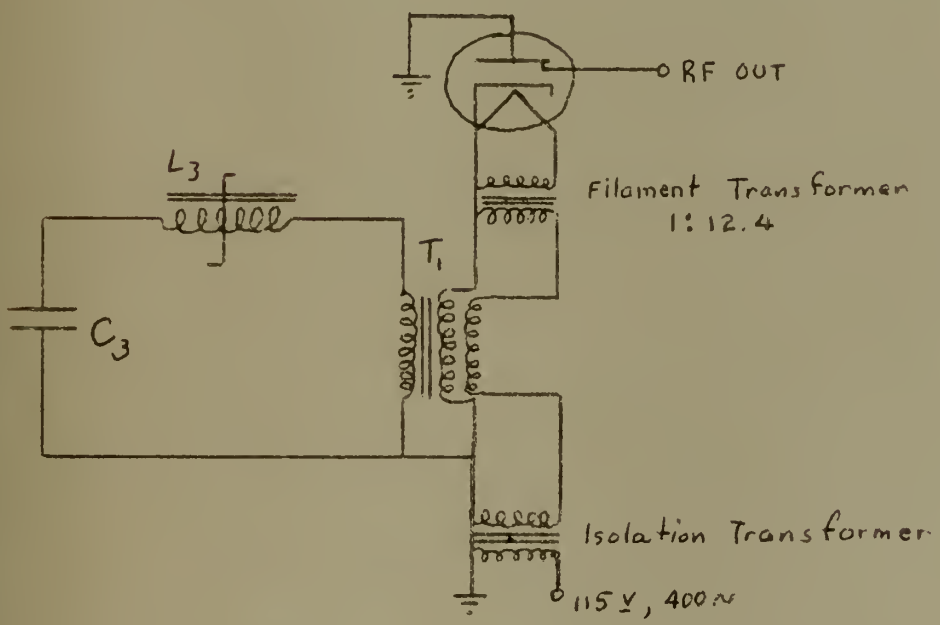


Figure 46. Schematic Diagram of Final Stage.

into account in this computation, as well as a decision on how far apart the two ends of the winding are to be. You can then, by substituting the numbers for the known quantities, such as the inside diameter (ID) and outside diameter (OD), and the circumference, write an equation involving the sum of these quantities, and solve for the $x_1$ of both the primary and the secondary. One of the basic premises is that the H's of the primary and secondary will be the same. A sample calculation of the above is included to illustrate the principle involved.

Taking into consideration the thickness of the insulation, case thickness, and the 1/32" thickness of the locking bands for the fins, we now have ID = 4.995"

OD = 8.993"

The loss of circumference due to 52 fins, (the number required by both primary and secondary) = 1.628"

Letting the superscript (p) indicate the primary winding, and the superscript (s) indicate the secondary, we have

$$A_1^p = (.1501)^2 \times 42.5 \times 2 = 1.917 \text{ in.}^2$$

$$A_2^p = .959 \text{ in.}^2$$

$$A_1^s = 0.1548 \text{ in.}^2 \qquad \& \; H_1^p = H_1^s$$

$$A_2^s = 0.0774 \text{ in.}^2$$

Now, $x_1^s = \frac{A_1^s}{A_1^p}$, $x_1^p = 0.0808\ x_1^p$ or $x_1^s = .0808\ x_1^p$

The total inside circumference = 15.69". Now write down the equation for the circumference in terms of $x_1$ and the number of bundles involved, also

allowing for the fins, and the spacing between the ends of the windings, in this case = 2.00".

This is: $49\ x_1^s + 1.628 + x_1^p + 2.000 = 15.69$

Then substituting for $x_1^s$, you can solve for the single unknown, $x_1^p$.

Therefore, $x_1^p = 2.43"$

$x_1^s = 0.197"$

Then, $H_1^p = H_2^s = 0.862"$

The other values of H and x can now be found.

As one end of the primary, and one end of the secondary are grounded, it is not necessary to separate both ends of the primary and secondary, but only the two high voltage leads. It is found, that due to the build up of the windings in each bundle, the separation, in this case, finally = 1.17". This is quite adequate for the voltages involved.

The material that is used to lock the fins into place has certain insulating properties, but this factor is considered as an additional safety factor, and is ignored in this development.

If the L (air core) is now recomputed from the above figures, it will be found, as is previously mentioned, that it is quite a bit in error. At this time, you also have an estimate of what degree of arc the windings will occupy, so that further refinement is now possible. It is now required that the complete design be redone, with these estimated factors taken into consideration. It may be necessary to do this three or possibly four times, before a final result is obtained.

Without going through this complete procedure again, the final design as arrived at by this writer follows. Note that it is somewhat different

than the one above, due to these changes that have occurred in the dimensions.

7. First stage pulsactor design.

$N_1 = 1800$ turns

$N_o = 24$ turns

$A = 34.5\ cm^2$

$h = 2.31"$

Number of turns per bundle $= 37$

Number of bundles $= 49$ in the secondary, less 13 turns on the last bundle.

$d_1 = 5.00"$ after winding

$d_2 = 10.83"$ after winding

$h = 3.159"$ after winding

$L_1$ (air core) $= 48.7 \times 10^{-3}$ henries. ($45.4 \times 10^{-3}$ henries was desired)

the $f_1$ as finally obtained will be $= 4.15 \times 10^3$ cps.

then $i_1$ (peak) $= 19.1$ amps. (From equation VII, page 40)

$\ell_1$ (mean path length of the core) $= 25.5$ inches.

Primary winding - AWG #7 Formex, 0.6 ohms/1000'

Secondary winding - AWG #20 Formex, 13.5 ohms/1000'

8. Computation of core loss.

$W = A \times J \times PRF \times \ell = (25.5)(2.54)(34.5)(1.5 \times 10^{-4})(400) = 134$ watts.

Where $A = cm^2$

$J$ = Joules/c.c./cycle. (From the graph, Figure 47.)

PRF = pulses/sec

$\ell$ = mean path length, cm.

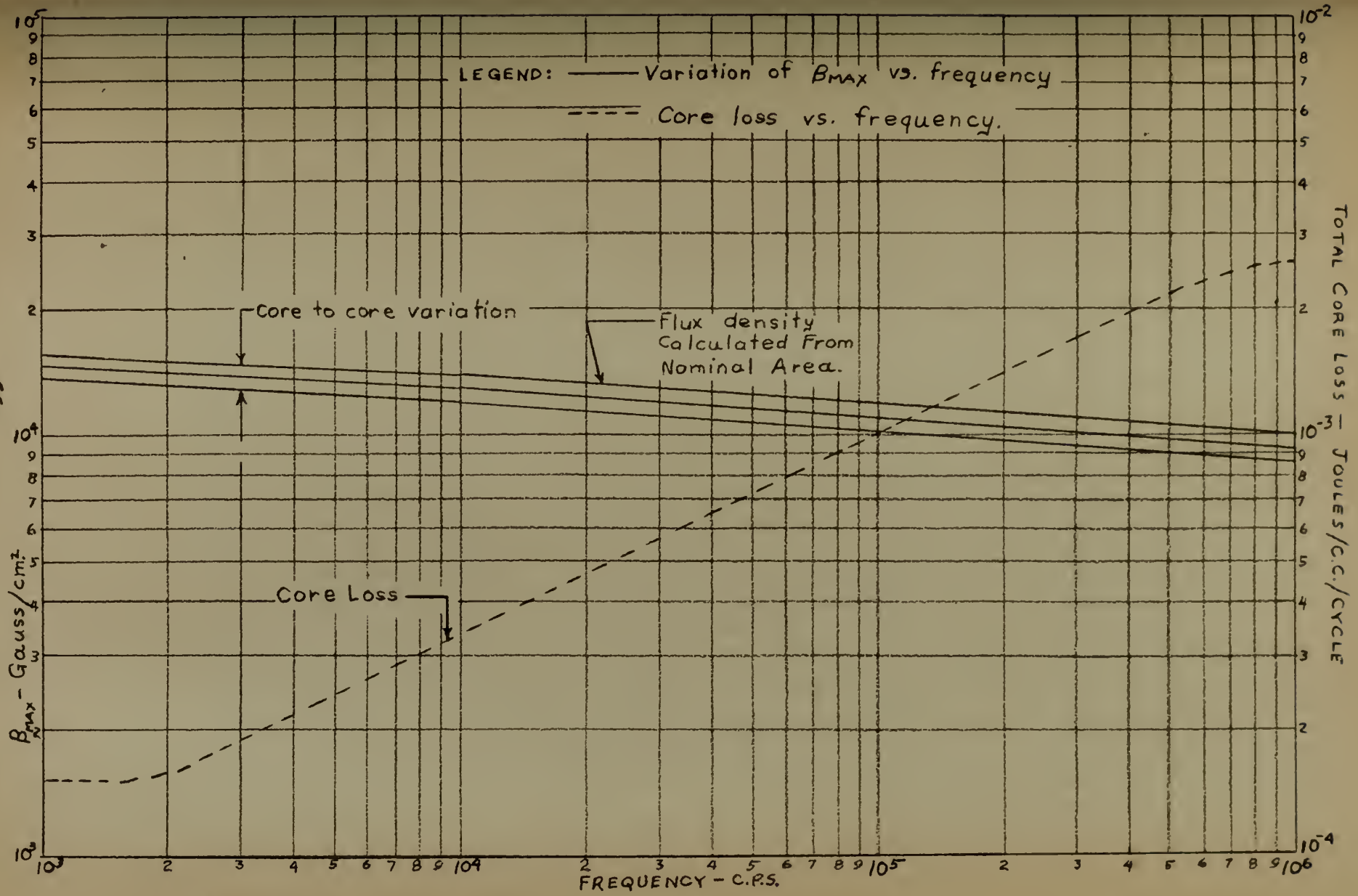


FIGURE 47. $B_{MAX}$ vs. Frequency, and Core Loss vs. Frequency.

9. Second Stage.

Using the constants of the circuit as given above, the computation of the second stage is now feasable.

$$f_2 = f_1 \frac{1}{\sqrt[3]{2\tau f_o}} = 3.548 \times 10^4 \text{ cps}$$

From the graph, Figure 47, $\beta$ max $= 1.2 \times 10^4$ gauss/cm$^2$.

$L_2$ (air core) $= 0.67 \times 10^{-3}$ henries. (From equation XI, page 28.) At this point we once again arrive at the point where it becomes necessary to compute the size of the core. As an aid to production, let us assume that the same size core will be used in the second stage as in the first. In that case, h, $d_1$, and $d_2$ are the same as in the first stage pulsactor.

$N_2 = 189$ turns, $L_2$ (air core) $= 336 \times 10^{-6}$ henries.

This $L_2$ is quite a bit different than is what is computed above, which means that a different frequency multiplication is used.

The new $f_2 = 5.05 \times 10^4$ cps. This is a frequency multiplication of 12.2 over $f_1$. It is not advisable to attempt a greater multiplication than 15, it has been found in practice.

$I_{2o} = 0.925 + 9.24 = 10.17$ amps RMS.

Wire diameter $= \sqrt{250} \times \sqrt{10.17} = 50.36$ mils.

Therefore it will be necessary to use AWG #16 wire, insulated diameter $= 53.7$ mils. A quick computation shows that this can be wound in a single layer on the core, with plenty of separation between the ends of the windings to prevent voltage breakdown.

10. Core loss in the second stage.

$W_2 = 191.28$ watts.

11. Third Stage

The following data is obtained from the magnetron characteristics.

$R_{mag} = 724$ ohms $\qquad f_2 = 5.05 \times 10^4$ cps

$\tau = 2$ micro-secs $\qquad L_2 = 336 \times 10^{-6}$ henries

$v_3 = 20.7 \times 10^3$ volts

As $\tau = 3.4 \frac{L_3}{R_c}$ and $\frac{R_c}{2L_3} = \frac{1}{\sqrt{L_3 C}}$ or $R_c = 2\sqrt{\frac{L_3}{C}}$

therefore, $\tau = 1.7\sqrt{L_3 C}$

$$\therefore L_{3\,TOTAL} = 0.345 \frac{\tau^2}{C}$$

and $L_3$ (total) $= 23 \times 10^{-6}$ henries

$$R_c = 2\sqrt{\frac{23 \times 10^{-6}}{.06 \times 10^{-6}}} = 39 \text{ ohms}$$

and $n^2 = \frac{R_{mag}}{R_c} = 18.5$

then $n = 4.3$. Initially it was assumed that $n = 4$, so this is within reasonable limits.

Now $L_3$ is divided between $L_3$ and the leakage L of $T_1$. It will be assumed that $L_3$ (total) = 1/2 of $L_3$ (total).

or $L_3 = 11.5 \times 10^{-6}$ henries

Now, $N_3 A_3 = \frac{v_3}{2} \frac{1}{4 B_{MAX} f_2} 10^8 = 441.$

Once more it becomes necessary to compute a particular core for this third stage. However, when the K of the core is computed, it is found that case #50182, 4 mil core, as listed in "Magnetics Inc." catalogue TWC-100, will be able to be used. From this,

$A = 8.71$ Cm$^2$ $\qquad d_2 = 6.825$"

$h = 1.826$" $\qquad d_1 = 4.174$"

Mean path length = 43.89 cm.

The above figures include the insulating tape thickness.

Then $L_3$ (air core) = $11.65 \times 10^{-6}$ henries. This is very close to that required, so this case will be used.

The pulse transformer, $T_1$, should now have $(23 - 11.65)10^{-6}$ henries of leakage inductance. This is 11.35 micro-henries. The number of degrees of arc of winding is estimated at 117°.

12. Design of the pulse transformer.

$L_t = 11.35 \times 10^{-6}$ henries

$\tau = 2 \times 10^{-6}$ seconds

PRF = 400

$\beta_{MAX} = 9.6 \times 10^3$ gauss/ $cm^2$ (Figure 47)

n = 4.3

$R_{mag} = 724$ ohms

$R_c = 39.1$ ohms

$v_p = 14.45 \times 10^3$ volts

The factors listed above are the specifications that must be met in this design.

Referring to Equation XIX, page 46, note that,

$$L_D = 11.35 = N_p^2 \times 10^{-2} \left[ 1.17(k_p h_p \log\left(\frac{d_2}{d_1}\right)_p + k_s h_s \log\left(\frac{d_2}{d_1}\right)_s) - \frac{0.8\ A_{core}}{\ell} \right]$$

Assume $k_p = k_s = 1.1$

then, $$11.35 = N_p^2 \times 10^{-2} \left[ 1.29\ h_p \log\left(\frac{d_2}{d_1}\right)_p + h_s \log\left(\frac{d_2}{d_1}\right)_s - \frac{0.8\ A_{core}}{\ell} \right]$$

Also, $$2 \beta \max N_p A_p \times 10^{-8} = \frac{v_t \tau}{n} = 28.6 \times 10^{-3}$$

or, $N_p A_p = 164$ (This also uses a safety factor of 10%, to insure that NA will be enough to hold off the saturation point.)

Combining the two equations given above,

$$11.35 = 222 \times 1.29 \frac{h_p}{A_p^2} \log \left(\frac{d_2}{d_1}\right)_p + 222 \times 1.29 \frac{h_s}{A_p^2} \log \left(\frac{d_2}{d_1}\right)_s$$

$$- \frac{0.8 \quad (222)}{A \ell}$$

This then, is the working equation. Selection of h, $d_1$, $d_2$, and A must be made so as to satisfy the above equation. It develops into a case of trial and error for different size cores, to see which comes the closest to satisfying the above equation. It must again be emphasized that this will not necessarily result in a final design for the pulse transformer, but instead provides a starting point for laboratory "cut and try" methods of development of a final design. With this point firmly in mind, selection of a core is made.

After a trial and error selection of one or two cases, it is found that using a standard core #50182 as listed in "Magnetics Inc." catalog, will give the following results:

$N_t = 22.5$ turns

$h = 2.581"$ All of the dimensions include insulating

$d_2 = 7.580"$ tape wound around the case.

$d_1 = 3.419"$

This results in the leakage inductance, $L_D = 9.64 \times 10^{-6}$ henries. It was desired that $L_D = 11.35 \times 10^{-6}$ henries. However, this is within the limits that may be expected, so that this will provide a good starting point for further development of the pulse transformer.

Then, $N_{2_t} = 97$ turns.

Let us look at the volts per turn involved in this transformer.

It has been found that if the output side of the transformer opens up, reflecting the open circuit to the primary, you may expect the voltage rize on the secondary to go to about twice its normal value. As it is required to obtain $61.5 \times 10^3$ volts on the cathode of the secondary, it will be necessary to provide for twice that, or $123 \times 10^3$ volts protection for design purposes. The volts per turn is then = 1270 volts per turn. It is obvious that the normal Formex wire that has been used to date, with a voltage breakdown wire to wire of 500 volts will not be satisfactory for this transformer if the windings are to touch each other. By referring to General Electric's tables of wire, it is found that if HFG wire is used, it will provide insulation against breakdown of 1800 volts wire to wire. This then, is the wire selected to wind the pulse transformer.

Now compute the current that flows in the primary and secondary of the pulse transformer, so that the wire size can be selected.

$$I_{3rms} = 0.886\ v_3\ C \sqrt{\frac{PRF}{\tau}} = 15.6 \text{ amps}$$

$$I_{3rms}\ (\text{total}) = 0.925 + 15.6 = 16.5 \text{ amps}$$

It will then be necessary to use wire of diameter $= \sqrt{250} \times \sqrt{16.5}$ = 64.23 mils. AWG #13 with HFG insulation will then be used.

Before computing the wire size of the secondary, first consider how the final stage is going to be connected to the magnetron.

Referring to the characteristics of this particular magnetron, it is found that the filaments require 85 amps at 7.3 to 9.3 volts. If the conventional bifalar type of winding were used, this would require the use of AWG #6 wire in the secondary of the final stage. This is prohib-

itively large, so that some different system must be used. One way is to use an isolation transformer from the 115 volt, 400 cps power supply. It will then be stepped down by a floating filament transformer to the required voltage. This is schematically illustrated in Figure 46. The design of the filament transformer is no small task in itself. This is not undertaken in this paper, but it is assumed that such a filament transformer may be designed. At any rate, by using this system, or one similar to it, the wire size in the secondary will be determined by the current required to heat the filaments plus the primary current transformed to the secondary. In this case, this results in being able to use AWG #17 wire, with HFG insulation.

Due to the space requirements of the winding of the pulse transformer, it is recommended that the insulation of the core from the windings, and the insulation between windings be spirally wound. Use the same insulating tape that has been previously listed, and spirally wind, so that there is never more than the necessary amount of tape between windings, or between windings and the core. Figure 48 shows how this final pulsactor may be wound. This is standard procedure for many pulse transformers.

13. <u>The charging choke.</u>

$$L_o = \frac{3}{(3\alpha^2 - 1) C \omega_o^2 \left(\frac{N_1}{N_o}\right)^2}$$

where $\alpha = 1.25$

$C = .06 \times 10^{-6}$

$\omega_o^2 = 64 \times 10^4$

$$\left(\frac{N_1}{N_o}\right)^2 = 5625$$

therefore, $L_o = 380 \times 10^{-6}$ henries

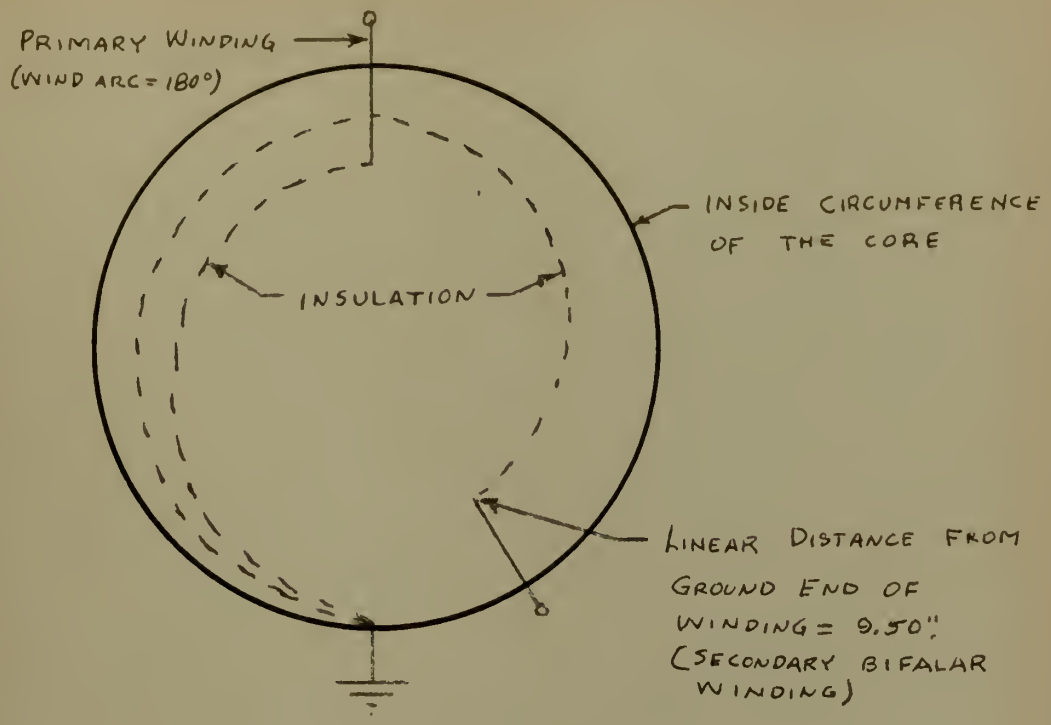


Figure 48. Spiral Wound Pulse Transformer.

14. Computation of bias current required.

The determination of the current required, and the value of the $L_4$ choke, depend on

1. $i_{avge} = \frac{3}{2}\left(\frac{N_b}{N_o}\right)\frac{E_o}{\omega_o L_4}$

2. $L_b = \frac{3}{c\,\omega_o^2}\left(\frac{N_b}{N_1}\right)^2$

Substituting the known factors into the above equations will result in,

$$N_b = 2920 \times \frac{1}{i_{avge.}}$$

Let us select the tap on the secondary, $N_b$ at 800 turns.

then $i_{avge.} = 3.65$ amps.

and $L_4 = 0.50$ henries.

A dry rectifier will deliver about one ampere per square inch of plate surface, when immersed in silicon oil. Using an adequate safety factor, to insure long life, $2\frac{1}{2}$ inch square plates are selected, with the total number of these plates being 15.

15. Estimate of Weight and Cube of the Completed Modulator.

The weight and cube of this modulator, can at best, only be estimated. The weight of the toroidal cores, and the copper involved in the windings can be computed quite accurately. However, the capacitors are a little more difficult to precisely determine. Also, there is some doubt as to how much silicone oil will be necessary to provide adequate cooling. It appears that some sort of heat exchange unit will also be required. The QK-428 magnetron itself requires liquid cooling of the anode, and a heat exchange unit is required for that purpose. Forced circulation of the oil is necessary if the heat exchange unit is used, and this problem

is not solved in this paper. One problem of using silicon oil is this forced circulation. Conventional pumps are not adequate, as sealing of rotary shafts, to prevent leaking when this type of liquid is being pumped, have not been devised, as of this date. One solution might be a bellows type of pump. It is also necessary to prevent foaming of the oil, and the formation of air bubbles.

An empirical equation for the volume of a condensor is given below. This volume is then used to compute the weight, using a density of 1.25.

$$\text{Capacitor Volume} = 40 \left[\frac{\text{Peak Volts}}{10^4}\right]^5 \times \left[\frac{\text{Capacitance}}{.02 \times 10^{-6}}\right] \text{ inches}^3$$

Using this above equation, in the case under question, where

Peak volts = $24.4 \times 10^3$ volts

Capacitance = $.06 \times 10^{-6}$ farads

Density = 1.25,

results in the weight of one capacitor = 46.6 lbs. Then for three of these capacitors, the weight would be = 140 lbs.

The Sprague Electric Company was consulted on this result, to ascertain if this was reasonable. On the basis of prior experience, this organization stated that the three capacitors would be in the vicinity of 221 lbs. This then, is the weight that is used in the estimate of the modulator.

In computing the weight of the toroids involved, the volume is first computed, and then a density of 8.25 is used to compute the weight. This will give a result that is very close to what the unit will finally weigh.

First and second stage pulsactors = 41 lbs.

Third stage pulsactor = 7 lbs.

Pulse transformer = 6 lbs.

The weight of wire required to wind each stage is then computed on the basis of the weight of wire as given in the wire tables. (For the size of the wire involved.)

Weight of copper for all stages = 1.6 lbs.

Weight of charging choke = 10 lbs.

Case weight = 15 lbs (estimated)

"Glastic" case to hold the units = 10 lbs. (estimated)

Three gallons of silicon oil = 24 lbs.

Weight of dry rectifier = 2 lbs.

In addition to the above, there will be a certain amount of piping for the oil to be transferred to the heat exchange unit, the heat exchange unit itself, and some type of pump to provide circulation of the oil. These quantities are intangibles that this writer is unable to assign a weight to.

The known, or estimated weights will add up to a total of 378.6 lbs., plus the unknowns as listed above.

It is of interest to compare this with the weight of the present conventional modulator unit as is in present service.

Power Supply for modulator = 261 lbs.

Modulator = 472 lbs.

Total = 733 lbs.

In addition to the above, there is also the magnetron itself, which weighs 70 lbs., and the heat exchange unit for cooling the anode of the magnetron, weight unknown. However, these two items are common to both

modulators. You can therefore save in the vicinity of 354 lbs. by using the magnetic modulator in place of the more orthodox type. This weight saving would be cut down by the weight of the additional heat exchange unit, pump, etc. as previously mentioned. However, it is believed by this writer that a considerable saving in weight will still result.

In one way, this comparison is unfair to the present modulator, in that it delivers two pulse widths at two PRF's, while the magnetic modulator is not so flexible. However, in light of the anticipated reliability of performance, a large improvement has still been made.

# BIBLIOGRAPHY

[1] Gardner and Barnes. Transients in Linear Systems, Volume I.

[2] Glasoe and Lebacqz. Pulse Generators. RadLab Series, Volume 5.

[3] Lee, Reuben. Electronic Transformers and Circuits.

[4] Massachusetts Institute of Technology. Principles of Radar.

[5] Melville, W. S. The Use of Saturable Reactors as Discharge Devices, For Pulse Generators. The Institution of Electrical Engineers, Paper #1034, page 185, Volume 98, Part 3, 1951.

[6] Terman. Radio Engineers' Handbook.

## APPENDIX A

## ANALYSIS OF AN EQUIVALENT CIRCUIT FOR A MAGNETRON LOAD

In the design criteria, as presented in this paper, the load on the modulator is assumed to be a pure resistance. This, of course, is far from what a magnetron load appears to the circuit. In an attempt to ascertain if the assumption of using a pure resistance for this load is justified, an analysis was made of an equivalent circuit for a magnetron. It is emphasized that this is not the only equivalent circuit, as others have been proposed.

Typical characteristics of a magnetron are given in Figure 49. The equivalent circuit of the magnetron is given in Figure 50. Note that the definitions of $R_1$, $R_2$, and $E_b$ are given in Figure 49.

The problem of analyzing the performance of the equivalent circuit of the magnetron, as illustrated above, will be accomplished in the steps as noted below.

1. Initially, the magnetron presents a load $R_1$ to the modulator.

2. When the magnetron starts to oscillate, the diode starts to conduct, presenting the network as shown. (S closes)

3. When the magnetron drops out of oscillation, the load on the circuit is again $R_1$. (S opens)

4. Comparison of the results of the first three steps will then be made to a circuit where the final stage is a critically damped resistance, $R_c$ as the load.

(Note: $R_1 > R_c > R_2$ )

In this analysis, the presence of the pulse transformer needlessly

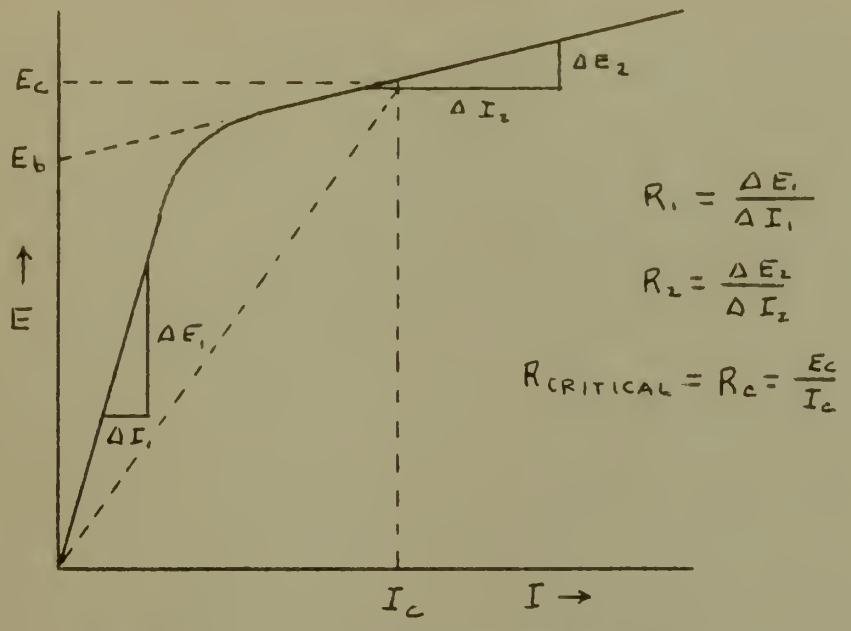


Figure 49. Magnetron Characteristic Curve.

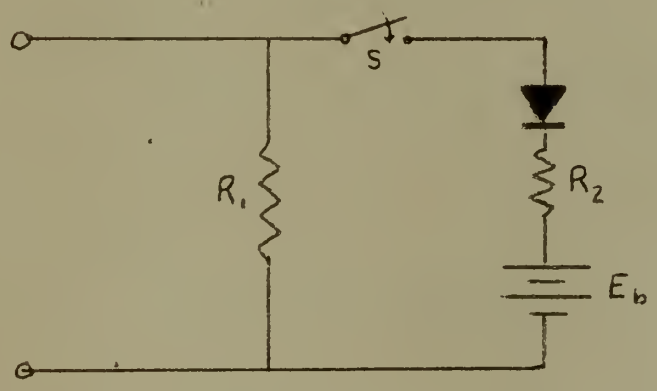


Figure 50. Equivalent Circuit of a Magnetron.

complicates the solution, without adding any additional information. Therefore, an ideal pulse transformer is assumed, and the resistances are transformed to the primary side of this transformer, resulting in the circuit to be analyzed as noted in Figure 51.

Assume that $E_b = 0.6$ V. This will vary with each individual case, but this is somewhere in the vicinity for a normal magnetron. Initially, switch S is considered to be open.

Therefore, $v_a = \frac{V R_1}{L}\left[\frac{\epsilon^{-\alpha t} - \epsilon^{-\gamma t}}{\gamma - \alpha}\right]$ .....XXII

Where, $\alpha = \frac{R_1}{2L} - \sqrt{\frac{R_1^2}{4L^2} - \omega^2}$ , $\omega^2 = \frac{1}{LC}$ ,

$\gamma = \frac{R_1}{2L} + \sqrt{\frac{R_1^2}{4L^2} - \omega^2}$

This analysis rapidly becomes a problem of high complexity to carry all the constants of the system in a general form. To show the final comparison, then, some circuit constants are now introduced. These value were taken from the circuit of a magnetic modulator that was built and tested to drive a 4J52 magnetron.

The circuit to be considered has the following parameters:

$L = 14 \times 10^{-6}$ henries

$C = .005 \times 10^{-6}$ farads

$R_1 = 298$ ohms, when transferred to the primary side of the pulse tran former.

$R_2 = 4.69$ ohms, when transferred to the primary side of the pulse transformer.

$E_b = 0.6$ V

V = V, the initial value of the voltage stored in C.

The voltage at point A for the equivalent circuit of the magnetron,

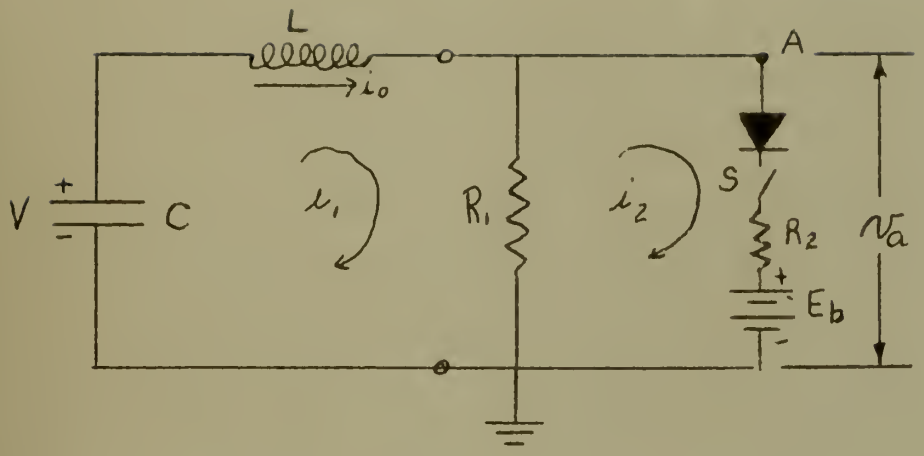


Figure 51. Circuit with Equivalent Circuit of Magnetron as a Load.

will now be computed for any time t. See Figure 51.

From equation XXII, $v_a = 1.07\ V\left[\epsilon^{-.69t} - \epsilon^{-20.59t}\right]$, where t is in microseconds.

Solving for $t_1$, the time when $v_a = 0.6V$, it is found that $t_1 = 0.043$ micro-seconds. At this time, $|i_o|$ the current in the coil, $= |0.002003\ V|$ and $v_1$, the voltage remaining on the capacitor, C is then $= 0.990V$.

Under these conditions, the switch s, is now considered to be closed.

Then, $i_2 = -9.845 \times 10^{-6}\ V\ [201.8 + 771.93\ \epsilon^{-.165t'} \sin(3.78t' + \psi)$ where $t'$ is in micro-seconds, and $\psi = -165^{\circ}$. Also, $t' = t - 0.043$.

Knowing $i_2$, $v_a$ can once again be computed for the period $t = 0.043$ micro-seconds to $t = 0.733$ micro-seconds. This second t is the time when $v_a$ once again is equal to 0.6 V. Therefore, at $t = 0.733$ micro-seconds, switch s opens, $|i_o| = |2.013 \times 10^{-3}\ V|$, and $v_2 = 0.245$ V.

Under the conditions as just stated,

$v_a = .2413\ V\epsilon^{-.69\ t''} + .3587\ V\epsilon^{-20.59\ t''}$

where $t'' = t - 0.733$ micro-seconds.

The results of the above analysis are plotted as $v_a$ vs. t, in Figure 52. Note that the period of oscillation of the magnetron is essentially defined as being confined to the "flat top" of the waveform of the voltage, $v_a$. From Figure 52, it is noted that this period of oscillation is $0.69 \times 10^{-6}$ seconds. The RF envelope of the 4J52 magnetron that was pulsed by this modulator unit, measured $0.73 \times 10^{-6}$ seconds.

For purposes of comparison of the equivalent circuit of the magnetron with the critically damped series RLC circuit, as used in the engineering design of the modulator unit, $v_a$, as computed in the design

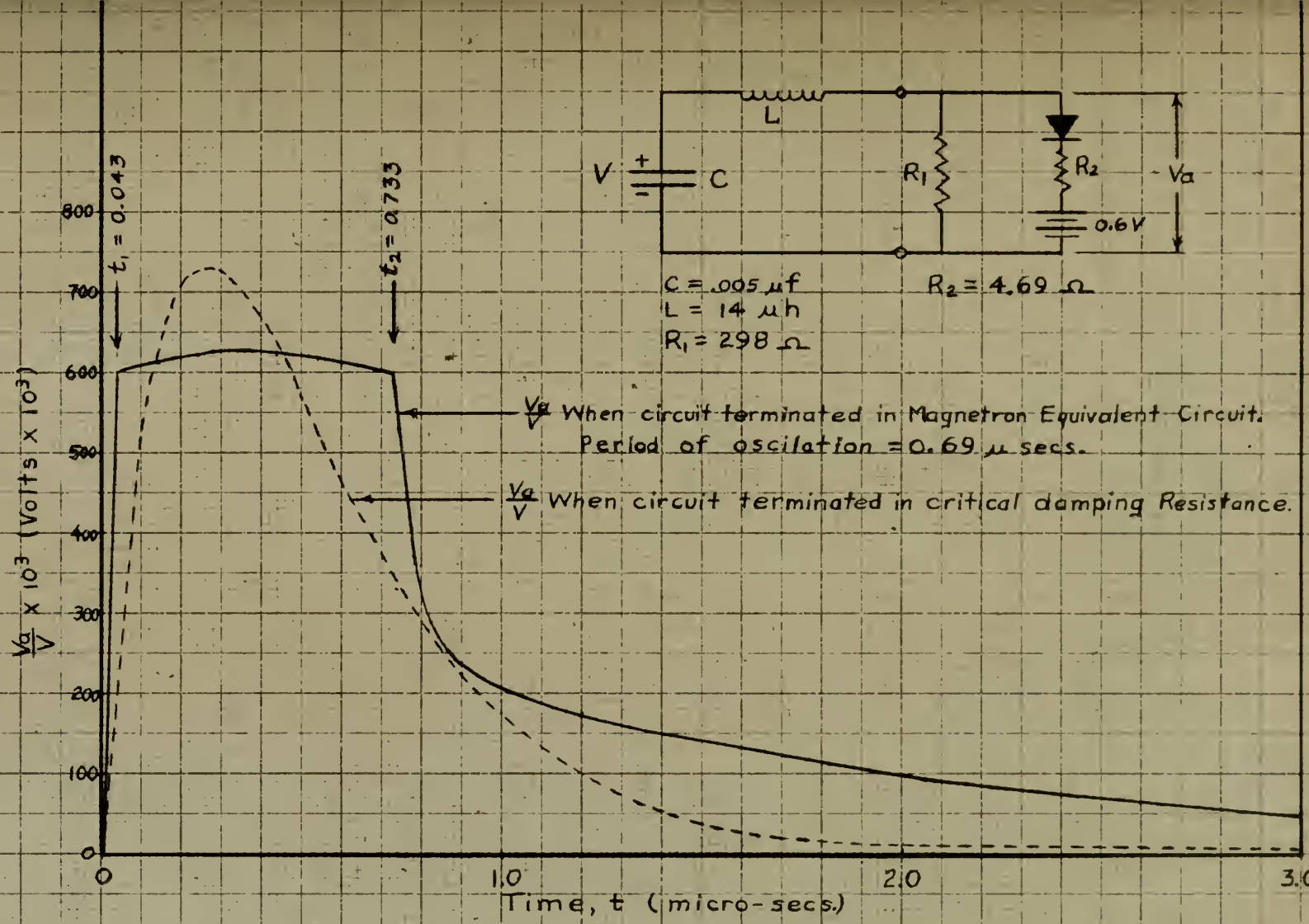


FIGURE 52. $\frac{V_a}{V}$ vs. Time in the circuit in Figure 51.

case, is included. This is,

$$v_a = 7.571\ V\ t\epsilon^{-3.78\ t}.$$

This is also plotted in Figure 52.

It is felt that the comparison of the two curves illustrates that it is feasable for design purposes to assume the load is a pure resistance.